Curcumin-Loaded Nanoparticles Potently Induce Adult Neurogenesis and Reverse Cognitive Deficits in Alzheimer's Disease Model *via* Canonical Wnt/β-Catenin Pathway

Shashi Kant Tiwari,[†,‡,⊥] Swati Agarwal,[†,‡,⊥] Brashket Seth,[†,‡] Anuradha Yadav,[†,‡] Saumya Nair,[†] Priyanka Bhatnagar,[§] Madhumita Karmakar,[†] Manisha Kumari,[§] Lalit Kumar Singh Chauhan,[†] Devendra Kumar Patel,[†,‡] Vikas Srivastava,[†,‡] Dhirendra Singh,[†] Shailendra Kumar Gupta,[†,‡] Anurag Tripathi,[†] Rajnish Kumar Chaturvedi,[†,‡,*] and Kailash Chand Gupta[†,‡,§,*]

[†]CSIR-Indian Institute of Toxicology Research (CSIR-IITR), 80 MG Marg, Lucknow 226001, India, [‡]Academy of Scientific and Innovative Research (AcSIR), New Delhi 110001, India, and [§]CSIR-Institute of Genomics & Integrative Biology (CSIR-IGIB), Mall Road, Delhi 110007, India. [⊥]S. K. Tiwari and S. Agarwal contributed equally to this work.

ABSTRACT Neurogenesis, a process of generation of new neurons, is reported to be reduced in several neurodegenerative disorders including Alzheimer's disease (AD). Induction of neurogenesis by targeting endogenous neural stem cells (NSC) could be a promising therapeutic approach to such diseases by influencing the brain self-regenerative capacity. Curcumin, a neuroprotective agent, has poor brain bioavailability. Herein, we report that curcumin-encapsulated PLGA nanoparticles (Cur-PLGA-NPs) potently induce NSC proliferation and neuronal differentiation *in vitro* and in the hippocampus and subventricular zone of adult rats, as compared to uncoated bulk curcumin. Cur-PLGA-NPs induce neurogenesis by internalization into the hippocampal NSC. Cur-PLGA-NPs significantly increase expression of genes involved in cell proliferation (reelin, nestin, and Pax6) and neuronal differentiation (neurogenin, neuroD1, neuregulin, neuroligin, and Stat3). Curcumin nanoparticles increase neuronal differentiation by activating the Wnt/β-catenin pathway, involved in regulation of neurogenesis. These nanoparticles caused enhanced nuclear translocation of β-catenin, decreased GSK-3β levels, and increased promoter activity of the TCF/LEF and cyclin-D1. Pharmacological and siRNA-mediated genetic inhibition of the Wnt pathway blocked neurogenesis-stimulating effects of curcumin. These nanoparticles reverse learning and memory impairments in an amyloid beta induced rat model of AD-like phenotypes, by inducing neurogenesis. *In silico* molecular docking studies suggest that curcumin interacts with Wif-1, Dkk, and GSK-3β. These results suggest that curcumin nanoparticles induce adult neurogenesis through activation of the canonical Wnt/β-catenin pathway and may offer a therapeutic approach to treating neurodegenerative diseases such as AD, by enhancing a brain self-repair mechanism.

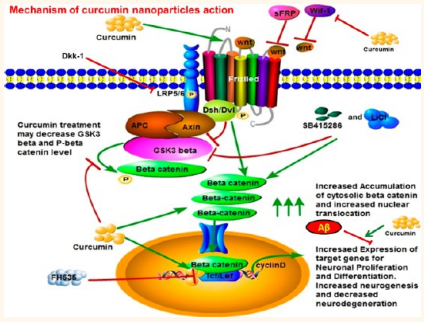

KEYWORDS: neural stem cells · neuronal differentiation · curcumin · neurodegenerative disorders · regenerative medicine · Alzheimer's disease · nanoparticles

In most mammalian species including humans, new neurons are generated throughout life from neural stem cells (NSC) by a process known as "neurogenesis".[1−3] NSC are multipotent and self-renewing cells that have the ability to generate all three types of cells in the brain. Neurogenesis takes place mainly in the two neurogenic brain regions the subventricular zone (SVZ) of the lateral ventricle and the subgranular zone (SGZ) of the hippocampus dentate gyrus.[1] Neurogenesis involves a balance between NSC proliferation, migration, differentiation to neurons, integration into the existing circuitry, and regulation of both olfaction- and hippocampus-dependent learning and memory processes.[1,4] All these processes take place within an appropriately regulated sequence and time frame, and any defect

* Address correspondence to (R. K. Chaturvedi) rajnish@iitr.res.in; (K. C. Gupta) kcgupta@iitr.res.in.

Received for review April 29, 2013 and accepted December 4, 2013.

Published online December 04, 2013
10.1021/nn405077y

may lead to neurodegenerative and neurodevelopmental disorders.[1,3]

Neurogenesis is negatively regulated by age, stress, and sleep deprivation and increased by caloric restriction, exercise, and physiological activation.[3] Several animal and clinical studies suggest reduced neurogenesis in neurodegenerative disorders such as Parkinson's disease (PD), Alzheimer's disease (AD), and Huntington's disease (HD).[1,5−9] Induction of neurogenesis through pharmacological and genetic approaches may reduce neurodegeneration and slow disease progression in neurodegenerative diseases.[10] Brain endogenous self-repair mechanisms may be increased by induction of adult neurogenesis to produce neurons and repair brain regions affected by neurodegenerative processes. Therefore, identification of molecules able to induce neurogenesis and deciphering the underlying cellular and molecular mechanisms of neuroregeneration may help in the development of regenerative medicines for the neurodegenerative disorders.

Curcumin, a natural polyphenol product derived from the rhizome of the Indian spice turmeric (*Curcuma longa*), possesses pleiotropic biological and pharmacological properties. Curcumin provides neuroprotection in cellular and animal models of neurodegenerative and neurological disorders including AD,[11,12] PD,[12,13] HD,[14] multiple sclerosis,[15] depression,[12] and schizophrenia.[16] Curcumin exerts neuroprotection due to its antioxidant properties and by activating the transcription factor Nrf2, a master regulator of the antioxidant response.[17] Curcumin inhibits amyloid beta (Aβ)-oligomerization and tau-phosphorylation in the brain and protects dopaminergic neurons against MPTP- and 6-OHDA-induced neurotoxicity.[18] Curcuminoids potentiate spatial memory in an Aβ-induced rat model of AD.[19] Curcumin promotes neurite outgrowth and proliferation of NSC *in vitro* and *in vivo* through activation of the ERK and MAP kinase pathways.[20,21] Curcumin treatment increases the number of neurons in chronically stressed rats[22] and cognition in aged rats.[23] In addition, it also plays a role in neurogenesis, synaptogenesis, and migration of neural progenitor cells *in vitro*.[24] Altogether, these studies suggest a potential neuroprotective role of curcumin.

However, the neuroprotective efficacy of curcumin is limited by its poor brain bioavailability due to poor absorption, rapid metabolism, systemic elimination, and limited blood brain barrier (BBB) permeability.[25] Several approaches have explored to increase curcumin bioavailability including the use of adjuvants such as piperine, liposomal curcumin, phospholipid curcumin complexes, and structural analogues of curcumin.[25] Biodegradable nanoparticle mediated delivery of curcumin may be an excellent approach to enhance its bioavailability in the brain, intracellular transport, and sustained and controlled release. Nanoparticles may increase the neuroprotective efficacy of curcumin and reduce the dose required and, due to the smaller size and high ingression power along with longer stability, can readily transmigrate across the BBB without compromising its integrity. Recent studies indicate that delivery of nanotized compound is more effective than its parent compound in the brain.[26−29]

Several neuroregulatory pathways such as transforming growth factor-β, Notch, and Wnt/β-catenin are involved in survival, proliferation, and differentiation of NSC in the brain during embryonic as well as adult neurogenesis. Among these, the Wnt/β-catenin pathway is mainly involved in the development of cortical and hippocampal neuroepithelium,[30] regulation of adult hippocampal neurogenesis, and self-renewal of neural stem/progenitor cells.[31−33] Wnt proteins/ligands are important extracellular factors that regulate NSC proliferation and differentiation.[34−37] Canonical Wnt/β-catenin signaling is altered or involved in the pathophysiology of AD and other neurodegenerative disorders.[36,37] Therefore induction of the canonical Wnt/β-catenin signaling could be a promising approach for the treatment of neurodegenerative disorders.[36]

Herein, we explored the neuroprotective efficacy of curcumin-encapsulated biodegradable poly(lactic-*co*-glycolic acid) (PLGA) nanoparticles (Cur-PLGA-NPs) compared to uncoated bulk curcumin (BC) on NSC proliferation and neuronal differentiation *in vitro* and in hippocampus and SVZ. We present a novel strategy to differentiate NSC into neurons using Cur-PLGA-NPs, which are able to release curcumin constantly and slowly. We also for the first time elucidated the molecular mechanisms underlying the canonical Wnt/β-catenin pathway activation and glycogen synthase kinase-3β (GSK-3β) inhibition by curcumin for the induction of neurogenesis. We studied the role of curcumin in enhancement of neurogenesis and its effects on behavior in an Aβ-induced rat model of learning and memory deficits and AD-like phenotype. We also identified novel molecular targets of curcumin using *in silico* prediction approaches. We observed that curcumin interacts with the Wnt inhibitor factor (Wif-1), Dickkopf (Dkk-1), and GSK-3β. We found that Cur-PLGA-NPs potently enhance NSC proliferation and neuronal differentiation and reverse Aβ-induced learning and memory deficits through activation of the canonical Wnt/β-catenin pathway.

RESULTS AND DISCUSSION

Preparation and Characterization of Cur-PLGA-NPs and *in Vitro* Release Profile of Curcumin. The present study involved the entrapment of curcumin into PLGA polymer. We used PLGA due to its biodegradable and biocompatible properties. Curcumin is insoluble in water, which greatly restricts its applications in experimental and clinical situations. Encapsulation of curcumin in PLGA leads to solubility of curcumin in water, and these nanoparticles monodisperse in water. Apart

A

Particles	Average Particle Size (nm)		Entrapment Efficiency	Zeta-potential
	DLS	TEM		
Cur-PLGA-NPs	200±20nm	30±5nm	~77±5%	-19±2.1 mV
FITC-PLGA -NPs	212±25 nm	35±7nm	~72±8%	-18±2.3 mV

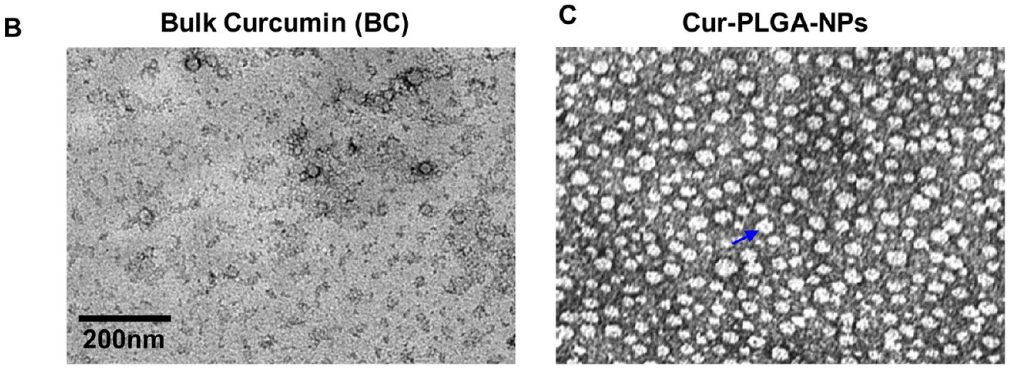

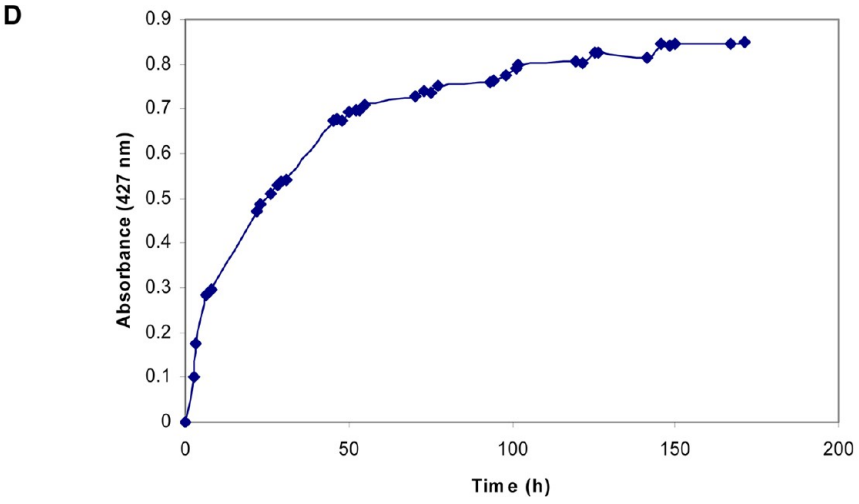

Figure 1. Characterization of bulk curcumin (BC) and curcumin encapsulated PLGA nanoparticles (Cur-PLGA-NPs). (A) Size, entrapment efficiency of curcumin, and zeta-potential of Cur-PLGA-NPs and FITC-tagged Cur-PLGA-NPs. Size was measured by dynamic laser light scattering (DLS) and transmission electron microscopy (TEM). (B, C) TEM photographs of BC (B) and Cur-PLGA-NPs (C). Scale bar: 200 nm. (D) Graph depicting *in vitro* release kinetics of curcumin from Cur-PLGA-NPs as percent drug release.

from the solubility, Cur-PLGA-NPs also exhibit green autofluorescence in a FITC filter. PLGA nanoparticles can cross the BBB and localize mainly in the hippocampus.[25] Several earlier studies used PLGA nanoparticles for the delivery of either retinoic acid or the antioxidant enzyme superoxide dismutase into the brain to induce neurogenesis and after cerebral ischemia.[38−40] Cur-PLGA-NPs were prepared using the emulsion solvent evaporation method.[25] After formulation of Cur-PLGA-NPs, we determined particle size, zeta-potential, entrapment efficiency, shape, and curcumin release profile (Figure 1A−D). The mean hydrodynamic diameter/particle size of Cur-PLGA-NPs as determined by dynamic laser light scattering (DLS) was 200 ± 20 nm, with a low polydispersity index (>0.3), indicating the formation of almost monodispersed nanoparticles (Figure 1A). The entrapment efficiency of curcumin in nanoparticles was found to be ~77 ± 5%. Thus, one milligram of Cur-PLGA-NPs consisted of 770 μg of curcumin. The surface charge of the Cur-PLGA-NPs was −19 ± 2.1 mV. The size and surface charge (zeta-potential) of the FITC-PLGA-NPs were 222 ± 25 nm and −18 ± 2.3 mV, respectively. The morphology of these nanoparticles was then characterized by transmission electron microscopy (TEM) (Figure 1B,C). The mean size of Cur-PLGA-NPs and FITC-Cur-PLGA-NPs as observed under TEM was 30 ± 5 nm and 35 ± 7 nm (Figure 1A). Cur-PLGA-NPs were mostly spherical in shape (Figure 1C). These results suggest that the size of Cur-PLGA-NPs was in the nanometer range. However, the size of

Cur-PLGA-NPs measured by both methods varied slightly, where increased size was observed by DLS as compared to TEM. This could be explained on the basis that DLS measures hydrodynamic diameter rather than the absolute diameter. A previous study also found an increase in the size of the nanoparticles when measured by DLS.[27]

The release kinetics of curcumin from the Cur-PLGA-NPs was studied for 8 days in 50% ethanol solution at 37 ± 2 °C, and we observed continuous curcumin release throughout this time. Also, it can be seen from the release graph that ~74% of the encapsulated curcumin was released in 7days (Figure 1D). The percent drug release was recorded to be fast and approximately linear until approximately 60% of the curcumin was released. Thereafter, a prolonged sustained release phase with varying release rates was observed.

Cur-PLGA-NPs Internalize into NSC Derived from Hippocampus. Neurogenesis takes place throughout adulthood mainly in the restricted neurogenic niches such as the hippocampus and SVZ from a highly specialized cell population known as NSC.[1−3] These NSC can be differentiated into neurons under specific cues and play a pivotal role in the maintenance of brain plasticity and integrity.[1−3] Brain regenerative ability or self-repair mechanisms can be specifically induced by targeting NSC of the hippocampus and/or SVZ. Several previous studies suggest that PEI- and PLGA-based nanoparticles can be internalized into adult neuronal cells[41] and SVZ-derived NSC,[39] respectively. In the present study, we evaluated the internalization and cellular uptake potential of Cur-PLGA-NPs into NSC. Cultures of NSC and neurospheres were exposed to FITC-Cur-PLGA-NPs for 24 h, and their intracellular internalization was studied by fluorescence microscopy and TEM analysis. We observed a few FITC-tagged nanoparticles internalized into the NSC and neurospheres 3 h post-treatment (data not shown). Twenty-four hours post-treatment, the majority of the FITC-tagged nanoparticles were found to be internalized into the cytoplasm of NSC and neurospheres (Figure 2A,B). FITC-Cur-PLGA-NPs were also present in the cytoplasm of Tuj1$^+$ neurons and GFAP$^+$ astrocytes, which were differentiated from NSC in culture (Supplementary Figure S2). This is in accordance with a study showing that FITC-retinoic acid PLGA nanoparticles can internalize into the NSC.[39] Another recent study showed neuronal uptake and neuroprotective effects of curcumin-loaded PLGA nanoparticles in human neuronal cells.[42] PLGA nanoparticles internalize into the cells mainly by clathrin-mediated endocytosis.[43] Next, cellular uptake of Cur-PLGA-NPs and FITC-Cur-PLGA-NPs was assessed by flow cytometric analysis (Figure 2C). The cellular uptake study involved analysis of the fluorescence intensity of the FITC-Cur-PLGA-NPs, showing fluorescence in the FITC channel. We observed increased cellular uptake of FITC-Cur-PLGA-NPs because of their higher mean fluorescence intensity (MFI) compared to Cur-PLGA-NPs. High MFI suggests localization and uptake of an increased number of FITC-tagged nanoparticles inside the NSC, while extracellular nanoparticles were washed off during processing. TEM analysis suggested that Cur-PLGA-NPs were distributed all over in the cytoplasm. Interestingly, several nanoparticles were also found localized into the nucleus, nuclear membrane, and mitochondrial membrane (Figure 2D).

Cur-PLGA-NPs Induce NSC Proliferation and Formation of Neurospheres *in Vitro*. Altogether, the above studies suggest that Cur-PLGA-NPs can internalize into the NSC and therefore can regulate their biological activities such as proliferation and differentiation. We next assessed the effects of different doses (0.001, 0.01, 0.1, 0.2, 0.5, 5, and 50 μM) of bulk curcumin and Cur-PLGA-NPs on NSC proliferation and viability by the MTT (Figure 3A) and the alamar blue reduction assay (Figure 3B). At 24 h post bulk curcumin treatment significantly increased proliferation was observed only at a dose of 0.5 μM, while higher doses (≥5 μM) significantly reduced the proliferation/viability (Figure 3A,B). We found no significant effects on cell viability by bulk curcumin up to 0.5 μM as compared to control cultures. We also found no significant effect on cell viability by empty PLGA-NPs at all the doses studied (data not shown). In contrast, Cur-PLGA-NPs significantly enhanced the NSC proliferation at doses as low as 0.001 μM, with the highest proliferation at 0.5 μM, which persisted even at high concentration (50 μM). Treatment with 0.001−50 μM Cur-PLGA-NPs significantly enhanced the cell viability as compared to bulk curcumin. We found 0.5 μM to be a noncytotoxic dose for both bulk curcumin and Cur-PLGA-NPs. It is clearly evident from Figure 3 that bulk curcumin activates NSC proliferation only at 0.5 μM as shown from almar blue reduction and the MTT assay. Curcumin-encapsulated nanoparticles showed significantly increased NSC proliferation even at much lower doses (0.001, 0.01, 0.1, and 0.2 μM), at which bulk curcumin showed no proliferation-enhancing effects (Figure 3A,B). This suggests that below a threshold level or very low doses of bulk curcumin did not enhance the NSC proliferation, while curcumin nanoparticles caused increased proliferation. Here curcumin nanoparticles showed a 50-fold increased efficacy to enhance NSC proliferation as compared to the same dose of bulk curcumin used. These results suggest that Cur-PLGA-NPs enhance proliferation at very low dose and were not cytotoxic even at high dose as compared to bulk curcumin. Therefore use of curcumin nanoparticles offers a greater dose advantage and reduced cytotoxicity as compared to bulk curcumin. Reduced cytotoxicity and enhanced cell proliferation could be due to the smaller size, increased cellular uptake, and high ingression power along with longer stability of curcumin nanoparticles. This could also be

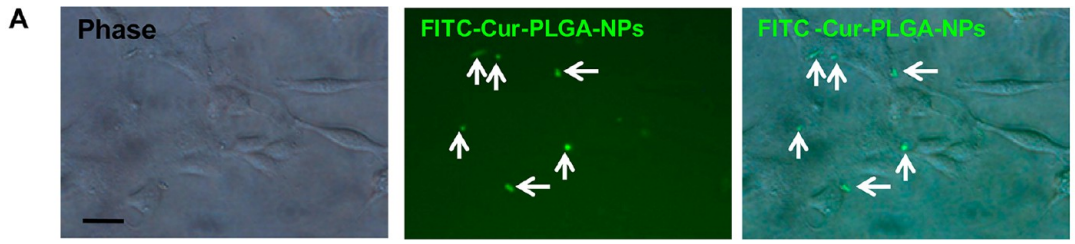

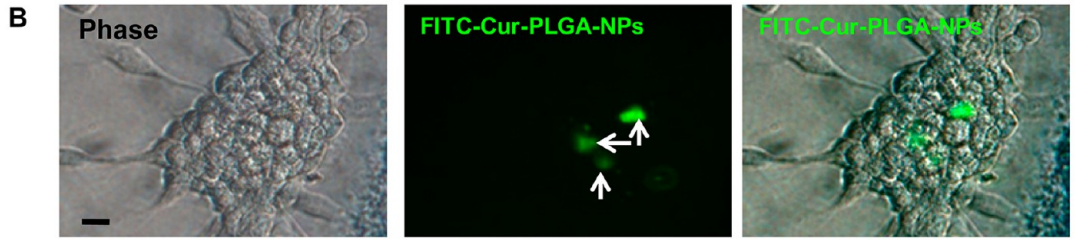

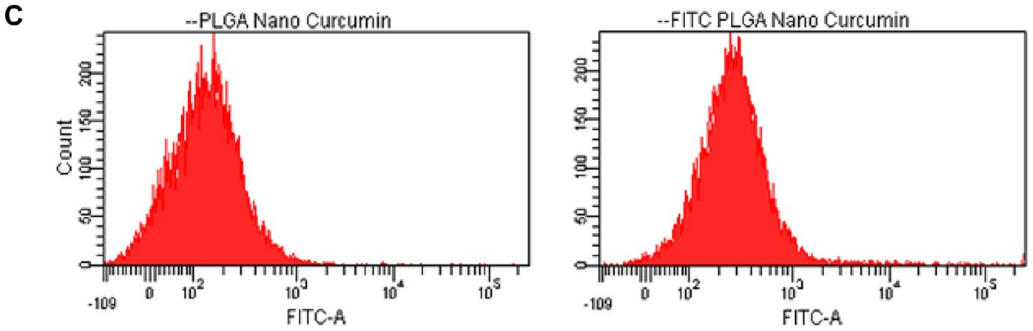

Groups	Mean Fluorescence Intensity
Cur-PLGA-NPs	224±10
FITC-Cur-PLGA-NPs	1048±68*

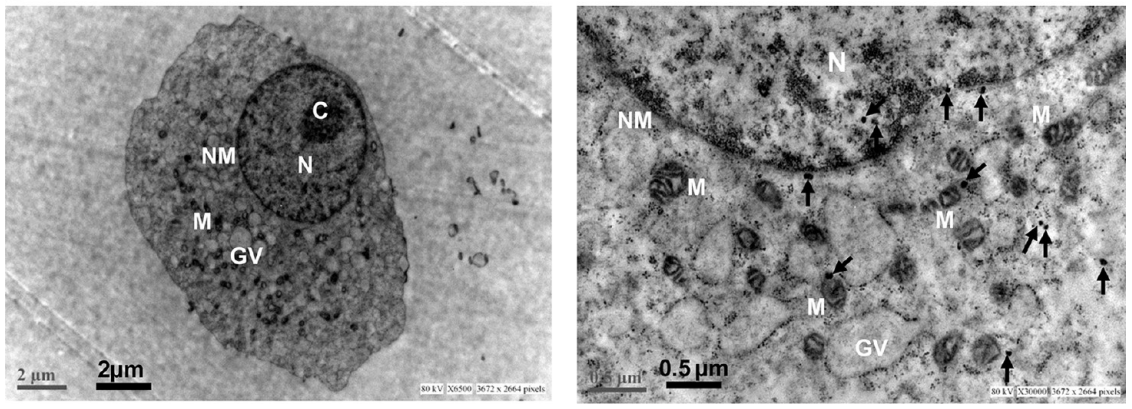

Figure 2. Cellular uptake of Cur-PLGA-NPs and FITC-Cur-PLGA-NPs. (A, B) Phase contrast and fluorescent images of the hippocampus-derived neural stem cells (NSC) (A) and neurospheres (B) after exposure to FITC-Cur-PLGA-NPs. Twenty-four hours post-treatment, FITC-Cur-PLGA-NPs were observed in the cytoplasm of the cells. Images are both at phase contrast and FITC channel. (Scale bar = 20 μm.) (C) Flow cytometry analysis in the FITC channel showing uptake of Cur-PLGA-NPs and FITC-PLGA-NPs in NSC by a shift in FITC mean fluorescence intensity ($n = 3$), *$p < 0.05$. (D) TEM photographs showing uptake of Cur-PLGA-NPs in the cytoplasm as well as their internalization in the nucleus of NSC. C = chromatin, N = nucleus, NM = nuclear membrane, M = mitochondria, GV = Golgi vesicles. Scale bars are 2 and 0.5 μm.

due to slow and sustained release of curcumin from the nanoparticles in the extracellular and intracellular space, while bulk curcumin may enhance cytotoxicity due to its presence in high concentration. A previous study also found curcumin-loaded PLGA nanoparticles nontoxic to human neuroblastoma cells.[42] A bromodeoxyuridine (BrdU) cell proliferation assay showed significantly increased NSC proliferation in neurospheres by Cur-PLGA-NPs at both the doses (0.1 and 0.5 μM), as compared to bulk curcumin (Figure 3C–E).

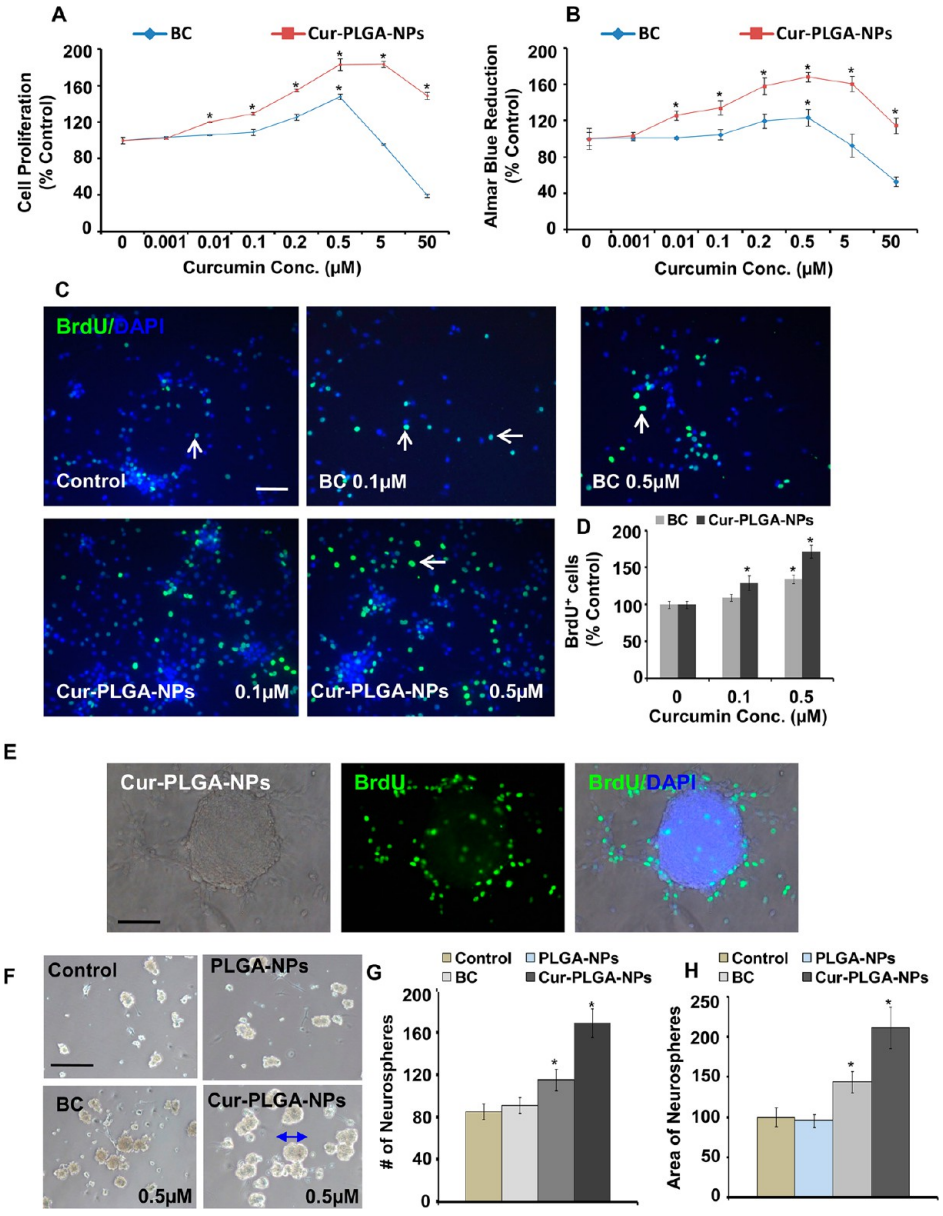

Figure 3. Cur-PLGA-NPs stimulate proliferation of the hippocampus-derived NSC and increase the number of primary neurospheres. (A, B) NSC derived from the hippocampus were seeded into 96-well culture plates and treated with the indicated concentrations of both bulk curcumin (BC) and Cur-PLGA-NPs for 24 h. The MTT assay and alamar blue assay were performed for cell proliferation analysis. Values are expressed as mean ± SEM (n = 3). *$p < 0.05$ *versus* BC. (C–E) BrdU immunoreactivity in NSC cultures (C) and neurospheres (E). BrdU immunoreactive cell quantification in the NSC cultures treated with curcumin (D). Graphical representation of percent increase of BrdU$^+$ cells labeled with the nuclear stain DAPI compared with the corresponding value for control as well as BC. Values are expressed as mean ± SEM (n = 3). *$p < 0.05$ *versus* control. Scale bar = 20 μm. (F) Representative phase-contrast photomicrographs of primary neurospheres derived from the hippocampus NSC treated with 0.5 μM each of BC, PLGA-NPs, and Cur-PLGA-NPs. (G, H) Quantification of the number of neurospheres (G) and area of neurospheres (H). Cur-PLGA-NP treatment caused a significant increase in the number and size of primary neurospheres as compared to control. Values are expressed as mean ± SEM (n = 3). *$p < 0.05$ *versus* control.

Co-localization of BrdU with DAPI in phase contrast and fluorescence photographs depicted the presence of BrdU$^+$ proliferating cells in the center and periphery of neurospheres treated with Cur-PLGA-NPs (Figure 3E and Supplementary Figure S3). Further, in order to assess whether Cur-PLGA-NPs show any effect on the number of the hippocampal multipotent NSC, we performed a neurosphere formation assay. Neurospheres are free-floating spherical clusters of NSC formed in the presence of specific mitotic growth factors. The number of clonal neurospheres *in vitro* is the measure of absolute putative stem cells *in vivo*. Gross morphology, size, and the number of neurospheres in all the groups were analyzed (Figure 3F–H). We observed a significantly increased number and size of primary and secondary clonal neurospheres treated with Cur-PLGA-NPs as compared to bulk curcumin. Empty PLGA-NPs did not show any effects on number and size of neurospheres.

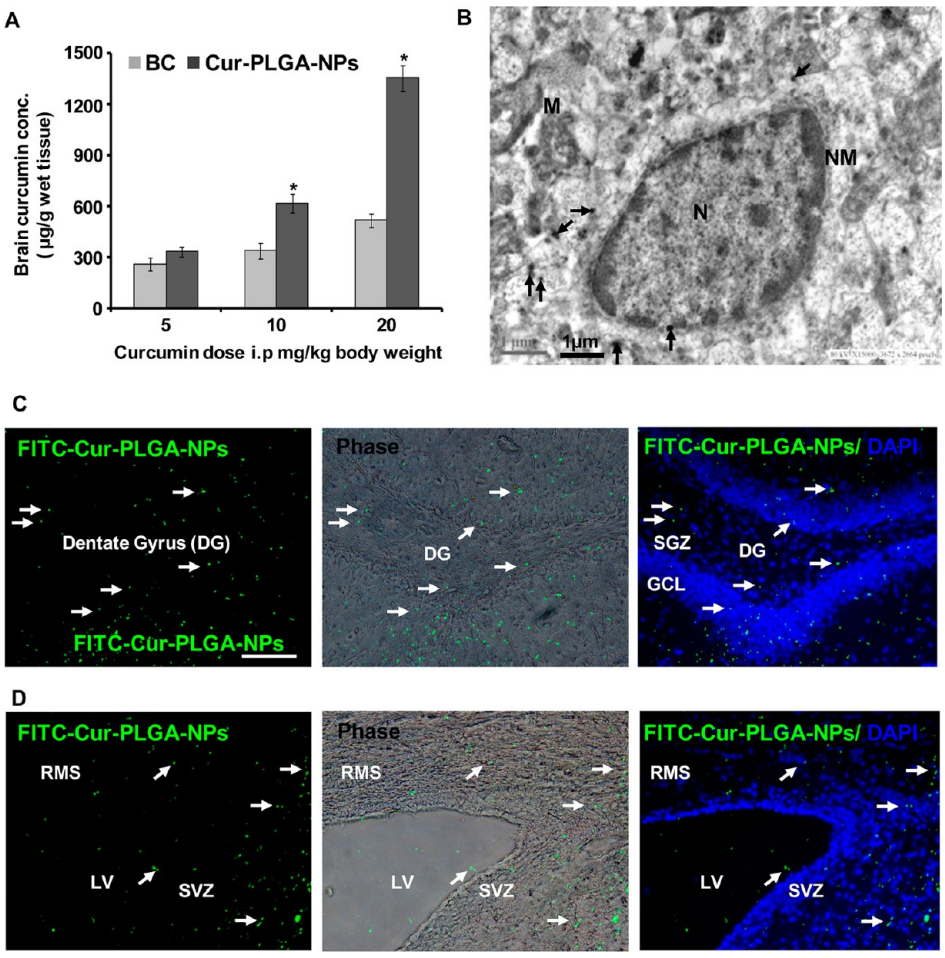

Figure 4. Cur-PLGA-NPs and FITC-Cur-PLGA-NPs internalize into the brain and enhance curcumin bioavailability. (A) Rats were treated with BC and Cur-PLGA-NPs (5, 10, 20 mg/kg body weight, ip). Levels of curcumin in the brain were measured by HPLC. Levels of curcumin were higher in the brain of rats treated with Cur-PLGA-NPs as compared to BC. Values are expressed as mean ± SEM (n = 6 rats/group). *p < 0.05 *versus* BC. (B) TEM photomicrograph of the hippocampus region showing accumulation of Cur-PLGA-NPs in the cytoplasm and internalization in the nucleus. N = nucleus, NM = nuclear membrane, M = mitochondria. Scale bar = 1 μm. (C, D) Fluorescence images at the FITC channel depict the uptake of FITC-Cur-PLGA-NPs in the hippocampus and the SVZ region of the rat brain and their co-localization with the nuclear stain DAPI. DG = dentate gyrus, SGZ = subgranular zone, GCL = granular cell layer, RMS = rostral migratory stream, LV = lateral ventricle. Scale bar = 100 μm.

These results suggest that Cur-PLGA-NP treatment increases the number of multipotent NSC and hence neurosphere formation.

Internalization, Cellular Uptake, and Bioavailability of Cur-PLGA-NPs in the Brain. Numerous studies suggest that due to antioxidant activity, curcumin acts as a neuroprotective agent. Curcumin can pass through the BBB because of its low molecular weight and hydrophobicity. However, the greatest challenge for curcumin to become a successful neuroprotective agent is its low brain bioavailability and high rate of metabolism. Moreover, curcumin is water insoluble, which restricts its use to a great extent for delivery into the brain. This limitation can be overcome by the synthesis of highly lipophilic curcumin nanoparticles, which can easily cross the BBB due to their small size, and sustained release of curcumin in the brain at a constant rate. In our study we found Cur-PLGA-NPs show slow and sustained release of the curcumin. We measured the bioavailability of curcumin in the brain, delivered through PLGA-NPs (Figure 4A). Rats were intraperitoneally treated with either bulk curcumin or Cur-PLGA-NPs (5, 10, and 20 mg/kg body weight), brains were collected, and curcumin levels were determined by HPLC analysis. The levels of curcumin in the 10 and 20 mg Cur-PLGA-NP treated groups were 2.1- and 2.8-fold increased, respectively, as compared to similar doses of bulk curcumin, suggesting increased bioavailability of curcumin in the brain (Figure 4A). TEM analysis of the hippocampus suggests internalization and the presence of Cur-PLGA-NPs in the entire cytoplasm and nucleus of the neuron (Figure 4B). We observed the presence of FITC-Cur-PLGA-NPs in the hippocampus and SVZ of the brain (Figure 4C,D). This is substantiated by an earlier study, in which curcumin-loaded PLGA nanoparticles were found to be localized to the hippocampus.[25] These results suggest that Cur-PLGA-NPs cross the BBB, are sustained, and slowly

release curcumin, leading to its increased bioavailability in the brain.

Cur-PLGA-NPs Enhance Cell Proliferation in the Hippocampus and SVZ of Adult Rats. To investigate the effects of Cur-PLGA-NPs on proliferation of NSC, we counted $BrdU^+$ cells in the dentate gyrus of the hippocampus and SVZ. BrdU is a synthetic thymidine analogue, which incorporates into DNA during cell replication, and is used for immunohistochemical detection of dividing cells. Rats received a daily single injection of BrdU (50 mg/kg body weight) for five consecutive days from postnatal day (PND 45−PND49) and were sacrificed 4 h after the last BrdU injection. Darkly stained, irregularly shaped, and compact $BrdU^+$ cells were observed in the hippocampus and SVZ (Figure 5A−C). A majority of the $BrdU^+$ cells were identified within the granular cell layer (GCL) and hilus regions of the dentate gyrus, with a small fraction also present in the molecular layer (ML). Treatment of Cur-PLGA-NPs significantly increased the number of $BrdU^+$ proliferating cells in the hippocampal GCL and hilus regions (Figure 5A,B) and SVZ (Figure 5C,D) as compared to bulk curcumin. Interestingly, Cur-PLGA-NPs also caused thickening of the SVZ lining (Figure 5C). Empty PLGA-NPs had no effects on cell proliferation in the hippocampus and SVZ. These results suggest that Cur-PLGA-NP treatment increases cell proliferation through slow and sustained release of curcumin in the hippocampus and SVZ.

Phosphorylation of histone-H3, a nucleosomal core protein, at the Ser10 residue during the G_2/M phase is a crucial mitotic event characteristic of proliferating cells.[44] The number of phospho-histone-$H3^+$ cells in the hippocampus was significantly up-regulated by the Cur-PLGA-NPs, suggesting the presence of cells undergoing mitosis (Figure 5E,F). Reelin, a secreted glycoprotein and extracellular matrix protein is involved in brain development, synaptic plasticity, learning and memory, NSC proliferation, neurosphere formation, and migration of neuroblasts.[45,46] Absence of reelin negatively affects the proliferation of NSC.[45] Decreased reelin-mediated signaling is associated with pathogenesis of several neurological and neurodegenerative disorders including AD and aging-related disorders.[46] The expression of reelin was significantly up-regulated by curcumin (Figure 5G), suggesting that increased proliferation of NSC observed in our study could be due to the enhanced expression of reelin in the hippocampus. We next studied the expression of the intermediate filament protein nestin, which is a molecular marker for multipotent NSC. Nestin is required for proliferation and self-renewal of NSC.[47] Expression of nestin was significantly increased (4.8-fold) by bulk curcumin; however it was increased more potently by Cur-PLGA-NPs (7.8-fold) (Figure 5G). Paired-domain-containing transcription factor (Pax6) is another gene strongly expressed in neural stem/progenitor cells and plays significant roles in brain patterning, neuronal specification, and neurogenesis.[48,49] Pax6 is highly expressed in the hippocampus and required for production and maintenance of progenitor cells for neurogenesis.[50,51] Pax6 expression was significantly up-regulated (1.2-fold) by bulk curcumin, which was increased more potently (3.9-fold) by the Cur-PLGA-NPs (Figure 5H). Pax6 expression was not altered by the empty PLGA-NPs (data not shown). This is the first time our study has demonstrated the positive effects of curcumin on reelin and Pax6 expression in the hippocampus.

Cur-PLGA-NPs Enhance Neuronal Differentiation and Expression of Neurogenic Genes. We next studied the effects of Cur-PLGA-NPs on neuronal differentiation. The fate and phenotype of newly born cells in the hippocampus and SVZ were assessed by co-labeling cells with BrdU/double cortin; DCX (a marker for immature newborn neurons), BrdU/NeuN (a marker of mature neurons), and BrdU/glial fibrillary acidic protein; GFAP (a marker for glial cells). An immunofluorescence co-localization study of BrdU/DCX showed that several $BrdU^+$ cells were co-localized with DCX in all the groups (Figure 6A). A significant effect of curcumin treatment on newborn neuron populations was observed. Bulk curcumin treatment caused a significant increase in BrdU/DCX co-labeled cells as compared to control rats (Figure 6A,B). However the increase in the number of BrdU/DCX co-labeled cells was more pronounced in Cur-PLGA-NP-treated rats. PLGA-NP treatment alone had no significant effects on neuronal differentiation in the hippocampus. This suggests that neurogenic differentiation potential was due to curcumin only, not the PLGA-NPs *per se*. These data indicate that curcumin increases neuronal differentiation of newborn proliferating cells. Furthermore, to investigate whether curcumin treatment has any effect on long-term survival and maturity of newborn neurons, we carried out co-localization studies of BrdU with NeuN. Cur-PLGA-NPs significantly increased the number of BrdU/NeuN co-labeled cells as compared to bulk curcumin (Figure 6C,D). PLGA-NP treatment alone did not produce any positive effects on the number of co-labeled cells. These results suggest that curcumin induces long-term survival and influence the phenotypic fate of newborn neurons. These results are substantiated by an earlier study, in which curcumin treatment produced significant inducing effects on neuronal differentiation.[21] Doublecortin is a marker for immature neurons and neuroblasts and is expressed specifically in migrating neuronal precursors/neuroblasts in the brain areas of continuous neurogenesis, *i.e.*, the hippocampus and the SVZ/olfactory bulb. We found that Cur-PLGA-NPs also increased the number of BrdU/DCX co-labeled neuroblasts in another neurogenic brain region, the SVZ (Figure 6E,F). Interestingly, we found a significant decrease in the number of BrdU/$GFAP^+$ cells by Cur-PLGA-NPs, which implies that the proliferating NSC followed the path

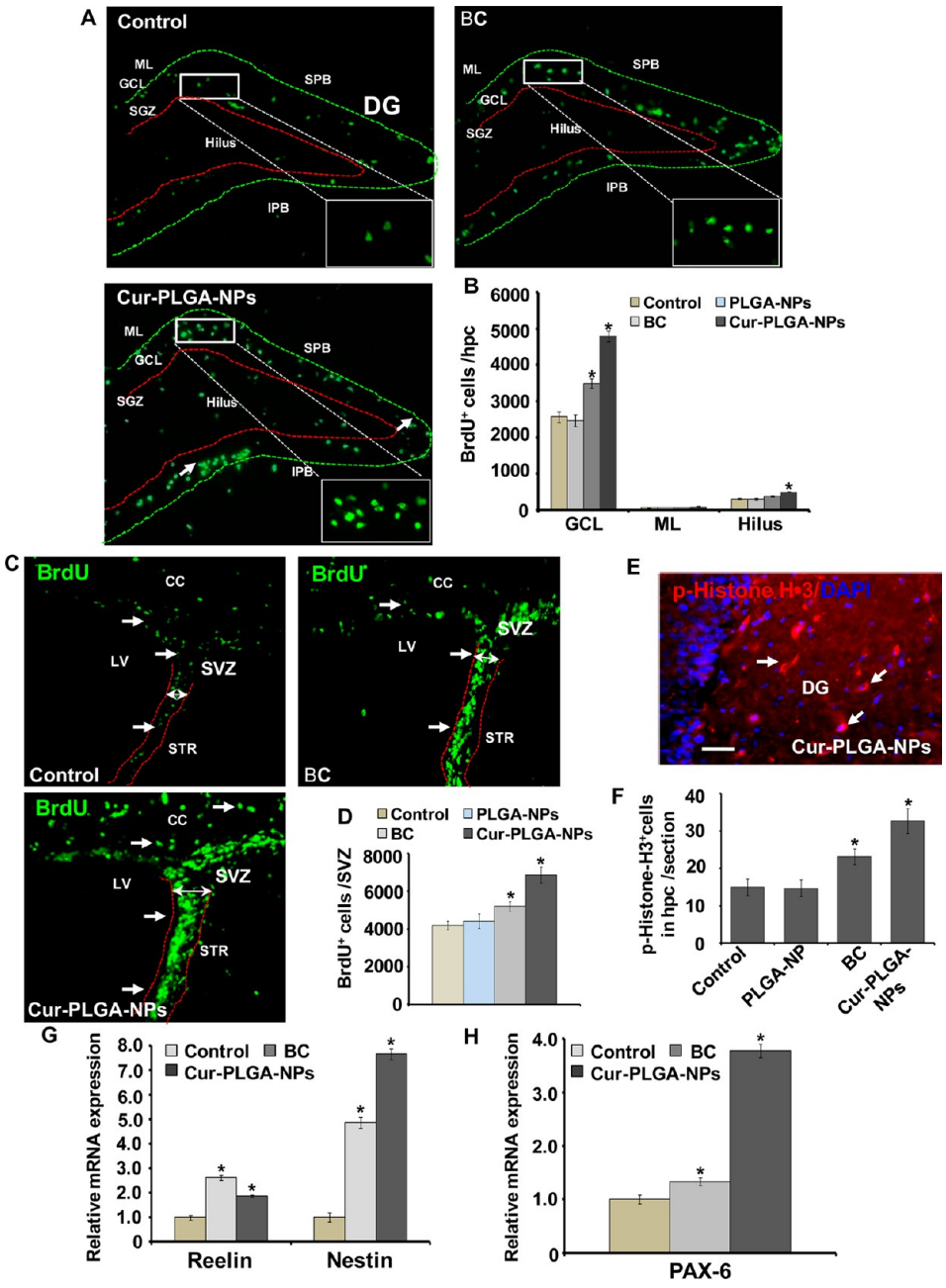

Figure 5. Cur-PLGA-NPs induce proliferation and self-renewal of NSC in the hippocampus and SVZ of adult rats. (A) Photomicrographs showing immunostaining of BrdU$^+$ cells in the dentate gyrus region of the hippocampus. BrdU$^+$ cells were mostly evident in the hilus and granular cell layer (GCL) regions, while a few BrdU$^+$ cells were also present in the molecular layer (ML) of the dentate gyrus in all the groups. Arrows indicate BrdU$^+$ cells. Inset shows typical morphology of darkly stained, irregular shaped, and compact BrdU$^+$ nuclei. SPB = suprapyramidal blade, IPB = infrapyramidal blade. Scale bar = 100 μm, 10 μm in inset. (B) Bar diagram showing quantitative analysis of the number of BrdU$^+$ cells in the GCL, hilus, and ML of the hippocampus. Values are expressed as mean ± SEM (n = 6 rats/group). *$p < 0.05$ *versus* BC. (C) BrdU$^+$ cells in the SVZ of control, BC-, and Cur-PLGA-NP-treated rats. Cur-PLGA-NP treatment caused an increased number of BrdU$^+$ cells and thickening of the SVZ lining containing NSC. (D) Quantification of BrdU$^+$ cells in the SVZ. Values are expressed as mean ± SEM (n = 6 rats/group). *$p < 0.05$ *versus* control. (E, F) Treatment of Cur-PLGA-NPs increases the number of phospho-histone-H3$^+$ granule neuroblasts in the hippocampus and SVZ. For analysis of proliferating cells, coronal sections from control, BC-, and Cur-PLGA-NP-treated rats were co-labeled with mitosis-specific marker phospho-histone-H3 and nuclear stain DAPI. (F) Quantitative analysis of hippocampal sections suggested a significant increase of phospho-histone-H3$^+$ mitotic cells in Cur-PLGA-NP-treated rats than control and BC. (G, H) Quantitative real-time PCR analysis was performed for relative mRNA expression of nestin (marker of NSC), reelin (an extracellular matrix protein required for proper migration and differentiation of NSC), and Pax6 in the hippocampus and normalized to β-actin. Values are expressed as mean ± SEM (n = 6 rats/group). *$p < 0.05$ *versus* control.

of becoming neurons rather than glial cells (Supplementary Figure S4). These results suggest that curcumin-NPs reduced glial differentiation in the hippocampus region. Further, it was found that

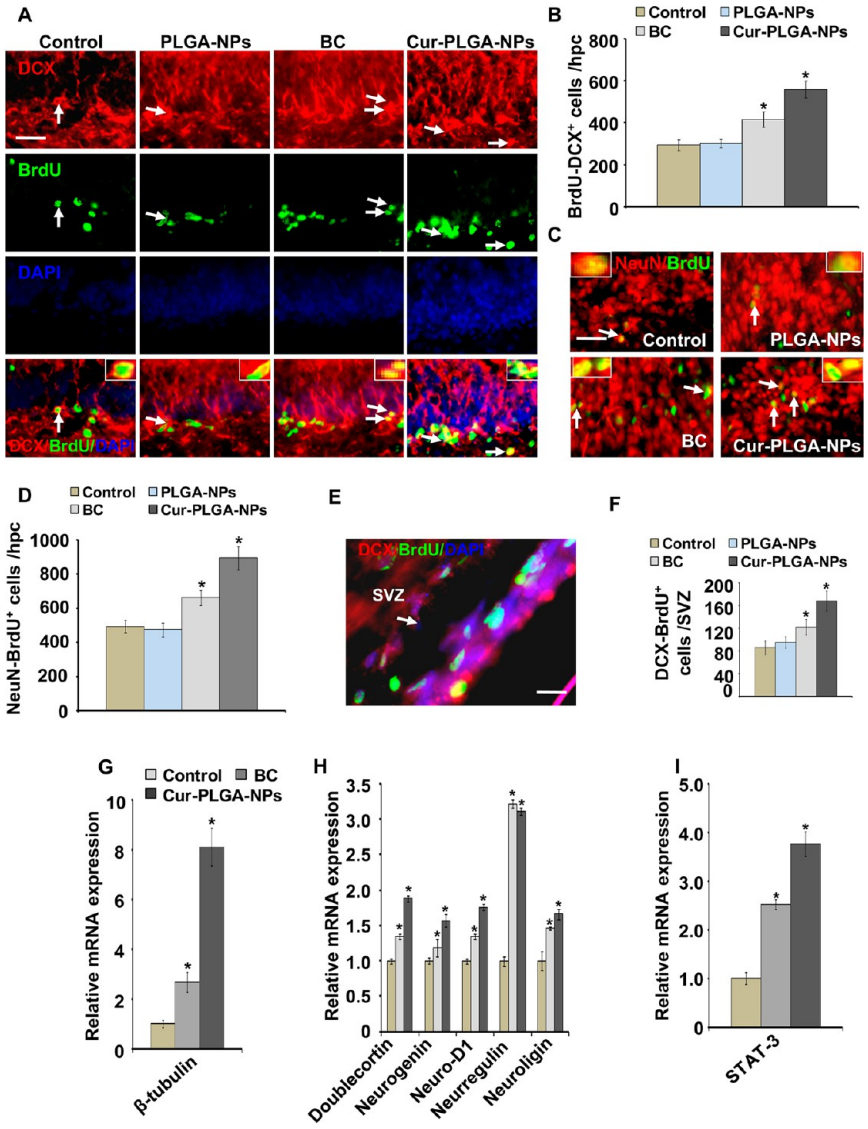

Figure 6. Cur-PLGA-NPs increase neuronal differentiation and adult neurogenesis in the hippocampus and SVZ of rats. (A) Double immunofluorescence analysis of newly born neurons co-labeled with DCX (red: marker for immature neurons) and BrdU (green; proliferating marker) in the dentate gyrus region of the hippocampus of PLGA-NP-, bulk-curcumin (BC)-, and Cur-PLGA-NP-treated rats. Arrows indicate $BrdU^+$ nuclei co-labeled with DCX. Inset showing higher magnification of BrdU/DCX co-labeled cells. Scale bar = 100 μm, and 10 μm in inset. (B) Quantitative analysis in the hippocampal sections showed a significantly increased number of immature neurons co-labeled with BrdU/DCX, suggesting increased neuronal differentiation in Cur-PLGA-NP-treated rats. Values are expressed as mean ± SEM (n = 6 rats/group). *$p < 0.05$ *versus* control. (C, D) Cells were double labeled with BrdU (green) and NeuN (red; mature neuronal marker) in the dentate gyrus region of the hippocampus. Arrows indicate $BrdU^+$ nuclei co-labeled with NeuN. (D) Quantification analysis suggested a significantly decreased number of mature neurons co-labeled with BrdU/NeuN in the hippocampus of Cur-PLGA-NP-treated rats. (E, F) Photomicrograph and quantitative analysis show a significantly increased number of DCX/BrdU co-labeled cells in the SVZ of Cur-PLGA-NP-treated rats. (G−I) Quantitative analysis by qRT-PCR suggested significantly increased relative mRNA expression of neurogenic genes and transcription factor Stat3 in the hippocampus of Cur-PLGA-NP-treated rats.

curcumin-NP treatment does not alter the morphology of glial cells in the hippocampus (Figure S4). Curcumin-NPs also enhanced neuronal differentiation and reduced glial differentiation in the hippocampus-derived NSC cultures (Supplementary Figure S5).

Next, we studied the specificity of the neurogenic potential of Cur-PLGA-NPs in the hippocampus. Rats were given a stereotaxic injection of bulk curcumin, FITC-PLGA-NPs, and FITC-Cur-PLGA-NPs directly into the hippocampus using stereotaxic coordinates. FITC-labeled NPs were present in the hippocampus of treated rats but not in control rats (data not shown). We found a significantly increased number of $NeuN^+$ neurons in the hippocampus of stereotaxically injected Cur-PLGA-NPs as compared to bulk curcumin (data not shown). Several neurogenic genes/transcription factors such as neurogenin, neurogenic differentiation 1 (neuroD1), neuregulin, neuroligin, and signal transducer and activator of transcription 3 (Stat3) regulate neurogenesis. Therefore expression of these genes was

studied in the hippocampus of all groups by qRT-PCR (Figure 6G–I). Bulk curcumin significantly up-regulated the expression of β-tubulin, neuroD1, DCX, neurogenin, neuroligin, and neuregulin and down-regulated the expression of Stat3. However, Cur-PLGA-NPs showed more pronounced effects on the expression of these genes. PLGA-NPs void of curcumin showed no effect on gene expression. Neurogenin belongs to family of basic helix–loop–helix (bHLH) transcription factors and is involved in neuronal differentiation, cell migration, and regulation of the cell cycle. Neurogenin in addition to promoting neurogenesis also inhibits astrocyte differentiation by inhibiting the Stat pathway.[52] Therefore, the observed increase in expression of neurogenin by treatment of Cur-PLGA-NPs may be the cause of the enhanced neuronal and reduced glial differentiation we observed in our study. Neurogenin also maintains progenitor cells in an undifferentiated state, allowing them to proliferate prior to maturation.[53] Thus, enhanced expression of neurogenin by Cur-PLGA-NPs may result in enhanced proliferation of NSC as observed in our study. The transcription factor Stat3 inhibits neurogenesis and promotes astrogliogenesis.[54,55] Inhibition of Stat3 leads to increased neurogenesis and reduced astrogliogenesis during differentiation of NSC. Stat3 expression was found to be decreased by Cur-PLGA-NPs, which might be responsible for increased neurogenesis and reduced gliogenesis. NeuroD1 induces terminal differentiation of newly synthesized hippocampal granule cells into the neuronal lineage during embryonic as well as adult neurogenesis.[53] Increased expression of neuroD1 due to Cur-PLGA-NPs treatment may result in increased neuronal differentiation and neuronal maturation. Overall, alterations in the expression of neurogenic genes/transcription factors result in increased neurogenesis, but the exact mechanism by which curcumin regulates the expression of these genes is still unknown and remains to be explored. These results suggest that Cur-PLGA-NPs significantly enhance neuronal differentiation in the hippocampus and the SVZ.

Cur-PLGA-NPs Activate Neuroregulatory Wnt/β-Catenin Signaling Pathway. Several external factors as well as intrinsic cellular pathways such as Notch, TGF-β/Smad, and Wnt are involved in regulation of proliferation and differentiation of NSC. Among these, the Wnt/β-catenin signaling regulates adult hippocampal neurogenesis and is involved in self-renewal of NSC/progenitor cells.[31–33] β-Catenin plays a central role in regulation of the Wnt/β-catenin canonical pathway. In the absence of Wnt ligands cytoplasmic β-catenin constitutively phosphorylates by GSK-3β for its ubiquitin-mediated proteasomal degradation. Activation of the Wnt signaling through Frizzled and LRP cell surface receptors leads to inhibition of GSK-3β and stabilization and decreased phosphorylation of cytoplasmic β-catenin. Stabilized β-catenin then translocates to the nucleus, binds to the transcription factor TCF/LEF, and activates the expression of responsive genes such as cyclin-D1. We assessed the mRNA expression and protein levels of the regulatory molecules, receptors, and transcription factors of the Wnt pathway (Figure 7A). We found Cur-PLGA-NPs significantly enhance the expression of Wnt3a, dishevelled, and Wnt receptors (Frizzled 1 and LRP-5/6) as compared to bulk curcumin (Figure 7A). However, expression of Wnt1 and Wnt5 was not affected (data not shown). Interestingly, the expression of Wnt3, LRP-5, and LEF was up-regulated by 7.9-fold, 8.5-fold, and 7.4-fold, respectively, by Cur-PLGA-NPs as compared to bulk curcumin. Cur-PLGA-NPs caused significantly decreased expression of Wif-1 and Dkk-1 as compared to bulk curcumin. Wif-1 is a protein that interacts with Wnt and inhibits the activation of the Wnt pathway. Similarly, Dkk is a negative regulator (antagonist) of the Wnt pathway and acts through inhibition of LRP-5/6, which is required for the activation of the Wnt pathway. A recent study suggests that expression of Dkk-1 increases with age, and reduced Dkk-1 expression leads to enhanced hippocampal neurogenesis and reduced cognitive deficits in mice.[56] Thus, increased expression and levels of Wnt3a by Cur-PLGA-NPs could also be explained on the basis of decreased expression of Wif-1 and Dkk-1 in the hippocampus. Curcumin nanoparticle treatment caused significantly decreased expression of genes involved in β-catenin destruction complex (Axin 1–2, APC, and GSK-3β) (Figure 7A). Curcumin nanoparticles also inhibited the expression of GSK-3β, a negative regulator of the Wnt/β-catenin pathway. Further, the expression of β-catenin, nuclear transcription factor (LEF), and cyclin-D1 was significantly enhanced by Cur-PLGA-NPs. Next, we studied the protein levels of Wnt3, dishevelled, TCF, GSK-3β, and β-catenin in the hippocampus (Figure 7B–D). We found curcumin nanoparticles significantly enhanced the levels of Wnt3, dishevelled, and TCF as compared to bulk curcumin. Empty PLGA-NPs did not show any effect on the levels of these proteins (data not shown). Wnt3 shortens cell cycle duration of neural progenitor cells, which ultimately promotes hippocampal neurogenesis.[57] Wnt3 is expressed in the hippocampal neurogenic region and regulates the population of newborn neurons.[58] Treatment of neural progenitor cells with Wnt3 increased the number of differentiating neurons, implicating the role of the Wnt pathway in neuronal differentiation.[35] Increased NSC proliferation and neuronal differentiation in our study can also be explained by the fact that Wnt3 concomitantly increases the number of proliferating cells and differentiated neurons.[57] Further, Wnt3 is involved in regulation of the canonical Wnt signaling, while Wnt5 regulates the noncanonical Wnt pathway. This suggests that curcumin activates the Wnt3-mediated canonical Wnt-β-catenin pathway. Wnt1 and Wnt5 are involved in regulation of the

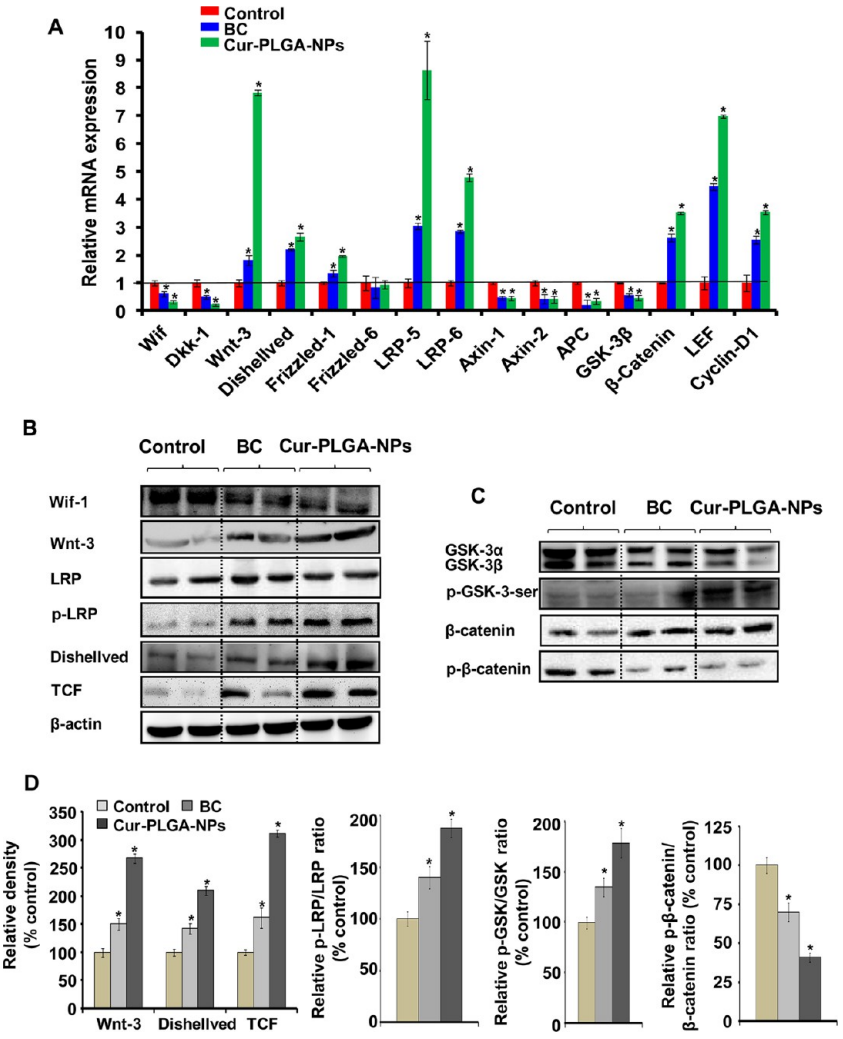

Figure 7. Cur-PLGA-NPs increase neurogenesis in the hippocampus through activation of the Wnt/β-catenin pathway. (A) Quantitative real-time PCR analysis was performed for relative mRNA expression of genes of the Wnt/β-catenin pathway in control, bulk curcumin (BC)-, and Cur-PLGA-NP-treated rats. β-Actin served as housekeeping gene for normalization. Values are expressed as mean $\pm$ SEM (n = 6 rats/group). *p < 0.05 *versus* control. (B, C) Western blot analysis of Wif-1, Wnt3a, LRP, p-LRP, dishevelled, TCF, GSK-3β, p-GSK-3β, β-catenin, and p-β-catenin protein levels in the hippocampus. Values were normalized to β-actin, used as a loading control. (D) Quantification of relative protein density after normalization with β-actin. Ratio of p-LRP/LRP, p-GSK-3β/GSK-3β was significantly increased and p-β-catenin/β-catenin significantly decreased in Cur-PLGA-NP-treated rats. Representative blots showing two samples from each group. Mean $\pm$ SEM (n = 6 rats/group). *p < 0.05 *versus* control.

midbrain dopaminergic neurons and neurogenesis in the substantia nigra and the olfactory bulb,[59−62] whereas Wnt3 regulates the hippocampal neurogenesis.[31,57,63,64] Wnt3a has a dominant role in hippocampal development, as deletion of Wnt3a (Wnt3a−/− mice) results in the absence of dentate gyrus formation.[65] Interestingly, it is shown that overexpression of Wnt3a alone can enhance hippocampal neurogenesis; on the other hand blockade of the Wnt signaling abolishes neurogenesis almost completely in the hippocampus.[31] Altogether these studies suggest that Wnt3a plays an important role in regulation and maintenance of hippocampal neurogenesis. Therefore activation of Wnt3 could be a promising approach to enhance hippocampal neurogenesis, a process that was found to be reduced in several neurodegenerative disorders including AD. Several neuroprotective agents were found to enhance neurogenesis through up-regulation of the canonical Wnt3a signaling in the brain.[66,67] Similarly, we also found curcumin-mediated activation of Wnt3a and neurogenesis in the hippocampus (Figure 7). These studies provide evidence that curcumin enhances the levels of Wnt3a in the hippocampus. A recent study also found that curcumin increased mRNA expression of Wnt10b, Wnt direct receptor Frizzled, and Wnt co-receptor LRP-5 in adipocytes, suggesting Wnt ligands and receptors of the canonical Wnt pathway are potential targets of curcumin.[68] Therefore, increased neurogenesis by Cur-PLGA-NPs could be due to enhancement of Wnt3 protein levels in the hippocampus. Increased expression and protein levels of Wnt3 and

resulting neurogenesis by Cur-PLGA-NPs as compared to bulk curcumin can be explained on the basis of slow and sustained release of curcumin from the nanoparticles; thus curcumin is available in the hippocampus for constant activation of Wnt3 and its downstream target genes.

Cur-PLGA-NPs Induce GSK-3β Phosphorylation, Reduce Phosphorylation of β-Catenin, and Increase Its Nuclear Translocation. GSK-3β is a serine/threonine kinase, which plays an important role in proliferation, differentiation, and neuronal survival and death. Phosphorylation of GSK-3β at Ser9 leads to its inactivation, causing accumulation of cytoplasmic β-catenin and activation of the Wnt/β-catenin pathway. The protein levels of GSK-3β were down-regulated, while its phosphorylation at Ser9 was significantly up-regulated by curcumin nanoparticles (Figure 7C,D). Densitometry analysis suggested a significantly increased ratio of p-GSK-3β/GSK-3β proteins by curcumin (Figure 7D). Here we found that curcumin may act as an inhibitor of GSK-3β by inducing its phosphorylation. Thus, we speculate that the enhanced neurogenesis observed in our study could be due to the decreased activity of GSK-3β. Earlier studies suggested that TWS119, a GSK-3β inhibitor, which phosphorylates β-catenin, induces selective differentiation of stem cells into neurons.[69,70] Another study found that curcumin activates the β-catenin pathway by inhibiting the activity of GSK-3β in neuronal cells.[71]

How GSK-3β is inhibited upon Wnt stimulation of cells has been a mystery for a long time; however now several recent studies have implicated the definitive role of Wnt and LRP in GSK-3β inhibition and activation of the canonical Wnt/β-catenin signaling. GSK-3β inhibition and β-catenin pathway activation through PI3K/Akt is very well established; however, recently several studies found involvement of Wnt in GSK-3β inhibition and β-catenin pathway activation. In order to study why p-GSK3β-ser was increased after curcumin treatment and how canonical Wnt signaling is involved in increased GSK-3β phosphorylation, we have assessed the LRP-5/6 phosphorylation. We have observed significantly increased mRNA expression and protein levels of Wnt3a, GSK-3β, and LRP-5/6 phosphorylation by curcumin in the hippocampus. GSK-3β inhibition by curcumin can be explained on the basis of a recent study, which suggests that phosphorylated cytoplasmic Wnt co-receptors LRP-5/6 cause direct competitive inhibition of the GSK-3β.[72] Canonical Wnt1 and Wnt3a bind to Frizzled and LRP-5/6.[73] Binding of Wnt to its co-receptors such as Frizzled and LRP-5/6 leads to phosphorylation of LRP-5/6 PPPSPxS motifs in the intracellular region.[72] The mechanism of canonical prototype Wnt3a-mediated phosphorylation of LRP-6 is well established.[73,74] Phosphorylated LRP directly binds to GSK-3β and causes its inhibition and subsequent activation of the canonical Wnt pathway.[72] LRP-6 also transduces the Wnt signal to inhibit GSK-3β-mediated phosphorylation of β-catenin, thus enhancing stabilization of β-catenin.[75] We found that curcumin causes phosphorylation of LRP-5/6, which may lead to inhibition of GSK-3β as observed in our study (Figure 7). Interestingly, Wnt3a induces inhibition of GSK-3β, stabilization of β-catenin, and stimulation of Wnt-dependent transcription.[76] These studies suggest that Wnt3a and LRP-5/6 directly inhibit GSK-3β and thus activate the canonical Wnt pathway.

β-Catenin, a substrate of GSK-3β, is another key molecule in the Wnt pathway. β-Catenin is also involved in neurogenesis in the adult brain.[77] Since GSK-3β activity negatively regulates the intracellular β-catenin levels, a decrease in GSK-3β levels by curcumin would be expected to result in an increase in the amount of β-catenin. Therefore, we measured the levels of β-catenin and its phosphorylation by GSK-3β. Cur-PLGA-NPs enhanced the levels of β-catenin and reduced its phosphorylation at the Ser 33/37/Thr41 residue by reducing the ratio of p-β-catenin/β-catenin (Figure 7C,D). As curcumin enhanced the levels and accumulation of β-catenin in the hippocampal cells, we further studied whether curcumin has any inducing effect on the mobilization of β-catenin into the nucleus. We assessed the nuclear translocation of β-catenin by co-immunofluorescence analysis of β-catenin/BrdU in the hippocampus and the SVZ (Figure 8A–C). PLGA-NP treatment alone did not produce any significant effect on β-catenin nuclear translocation. Cur-PLGA-NPs more potently enhanced the localization of β-catenin into the nucleus, as compared to bulk curcumin. Further, we found a significantly increased number of p-GSK-3β^+ cells and decreased number of p-β-catenin$^+$ cells in the hippocampus of Cur-PLGA-NP-treated rats (Figure 8D,E). These data suggested that Wnt-induced nuclear localization of β-catenin is enhanced by the Cur-PLGA-NPs.

Cur-PLGA-NPs Specifically Induce Neurogenesis through Activation of the Cyclin-D1 and TCF/LEF Promoter Activity. β-Catenin after nuclear localization associates with the TCF/LEF transcription factor, and then this complex binds to the promoter of Wnt-pathway genes such as cyclin-D1, *etc.*, to activate their expression. In order to assess the specific role of curcumin in the activation of the Wnt pathway, thereby inducing neurogenesis, we treated NSC cultures with the β-catenin/TCF inhibitor FH535, GSK-3β inhibitors SB-415286 and LiCl, and Wnt3a protein in the presence and absence of bulk curcumin and Cur-PLGA-NPs. After the respective treatments, we assessed the TCF/LEF and cyclin-D1 promoter luciferase activity (Figure 9A,B). Wnt3 protein, GSK-3β inhibitors, bulk curcumin, and Cur-PLGA-NPs significantly enhanced the TCF/LEF and cyclin-D1 promoter activity (Figure 9A,B). Interestingly, Cur-PLGA-NPs significantly increased the promoter activity when compared to the activity induced by the known GSK-3β inhibitor

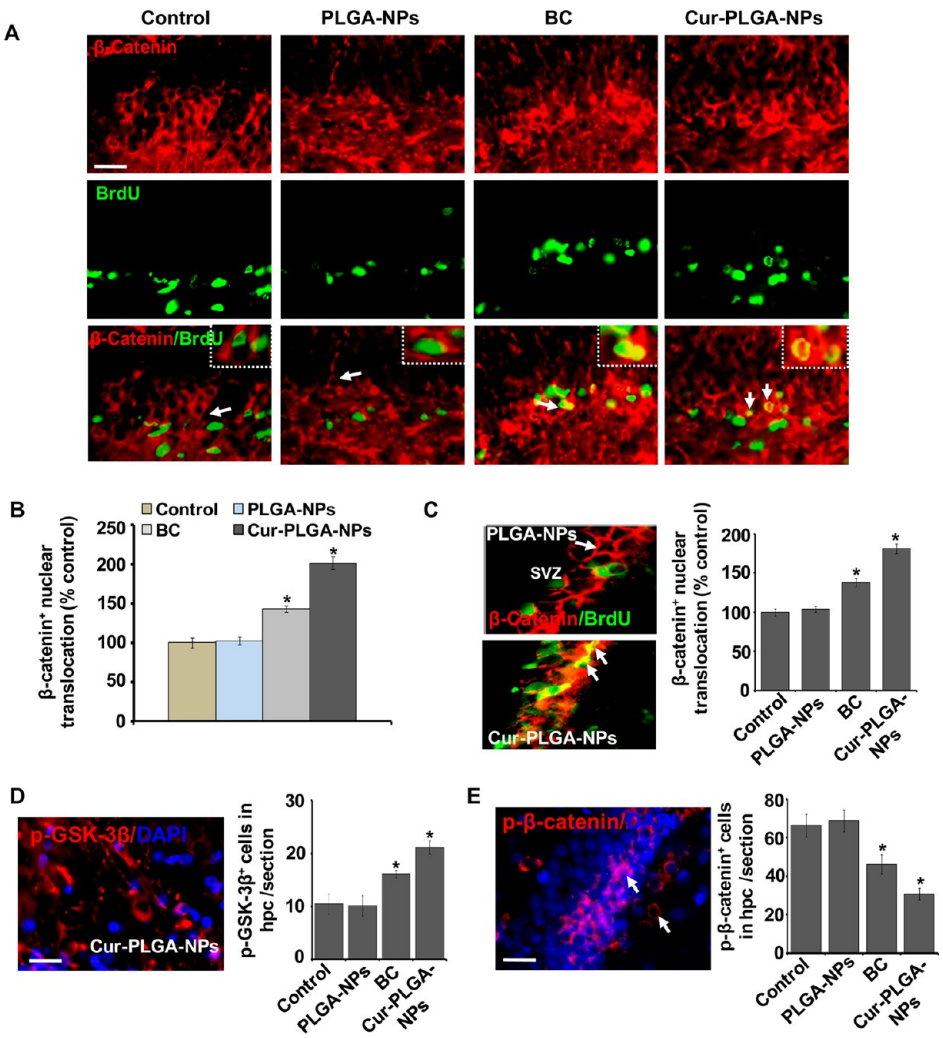

Figure 8. Cur-PLGA-NPs activate the Wnt/β-catenin pathway *via* enhancing nuclear localization of β-catenin and phosphorylation of GSK-3β in the hippocampus. (A) Immunofluorescence photomicrographs show cytoplasmic and nuclear localization of β-catenin (red), a key regulatory protein of the Wnt pathway, and its co-localization with BrdU (green) in the hippocampus of control, bulk curcumin (BC)-, PLGA-NP-, and Cur-PLGA-NP-treated rats. Arrows indicate BrdU$^+$ nuclei co-labeled with β-catenin. Inset shows higher magnification of BrdU/β-catenin co-labeled cells and nuclear localization of β-catenin. Scale bar = 100 μm, and 10 μm in inset. (B, C) Quantitative analysis shows that Cur-PLGA-NPs significantly enhance the percent nuclear translocation of β-catenin in the hippocampus (B) and SVZ (C). Values are expressed as mean $\pm$ SEM (n = 6 rats per group). *$p < 0.05$ *versus* control. (D, E) Quantification of p-GSK-3β (red) and p-β-catenin (red) positive cells with DAPI (blue) suggests a significant up-regulation of GSK-3β phosphorylation, and down-regulation of β-catenin phosphorylation by Cur-PLGA-NPs in the hippocampus.

SB-415286. This suggests that Cur-PLGA-NPs induce promoter activity through potent inhibition of GSK-3β. Co-treatment of curcumin with Wnt3 protein and GSK-3β inhibitors further enhanced the luciferase activity. Treatment with the β-catenin/TCF inhibitor FH535 resulted in significantly decreased promoter activity. NSC treatment with FH535 significantly abolished the promoter activity inducing ability of curcumin and Wnt3a protein, suggesting a specific role of the Wnt pathway in curcumin-mediated positive effects on neurogenesis. Pharmacological inhibition of the Wnt pathway by FH535 also inhibited neuronal differentiation in hippocampal-derived NSC cultures (Supplementary Figure S6). The mRNA expression of nestin, β-tubulin, and DCX was significantly decreased in NSC cultures co-treated with curcumin and FH535, suggesting decreased cell proliferation and neuronal differentiation (Supplementary Figure S6). Co-treatment of curcumin with Wnt pathway activator LiCl significantly enhanced the expression of these genes in NSC cultures (Supplementary Figure S6). These results revealed that curcumin can directly activate the Wnt/β-catenin signaling through Wnt and GSK-3β. Further, the ability of Cur-PLGA-NPs *vis-à-vis* curcumin to induce GSK-3β phosphorylation and activation of the cyclin-D1 and TCF/LEF promoter activity could be explained on the basis of intracellular localization of Cur-PLGA-NPs. Nanoparticles through cellular internalization release curcumin directly in the cytoplasm, where slowly and continuously released curcumin may interact with

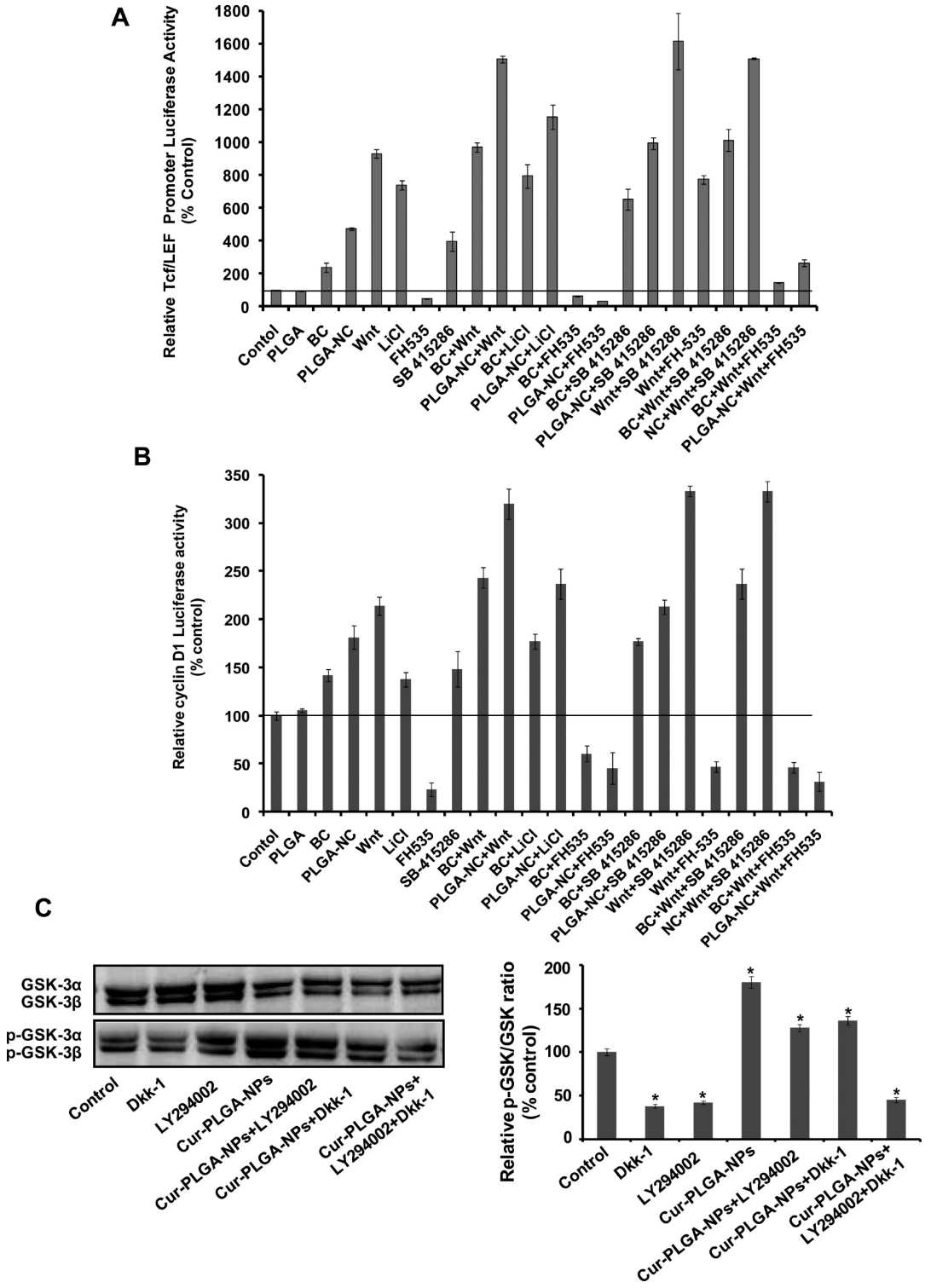

Figure 9. Cur-PLGA-NPs enhance cyclin-D1 and TCF/LEF promoter activity and inhibit GSK-3β in NSC *via* activation of the Wnt/β-catenin pathway. (A, B) The hippocampus-derived NSC were transfected with a cyclin-D1 promoter (1.88kb) construct linked to a luciferase reporter gene in the pGL3 vector and TCF/LEF promoter. NSC were treated with the β-catenin/TCF inhibitor FH535, GSK3-β inhibitors SB-415286 and LiCl, and Wnt3a protein in the presence and absence of bulk curcumin (BC) and Cur-PLGA-NPs. The luciferase activity is normalized to the firefly luminescence over renilla luminescence. Cur-PLGA-NPs significantly increased cyclin-D1 and TCF/LEF promoter activity in NSC. Values represent mean ± SEM of three experiments. (C) NSC cultures were treated with Wnt pathway inhibitor Dkk-1 and PI3K/Akt inhibitor LY294002 in the presence and absence of Cur-PLGA-NPs and bulk curcumin. After respective treatments, protein levels of GSK-3α/β and p-GSK-3α/β were studied. Values are expressed as mean ± SEM (n = 4). *p < 0.05 *versus* control.

GSK-3β and reduce its activity, leading to the activation of the cyclin-D1 and TCF/LEF promoter activity.

It is known that curcumin through PI3K/Akt inhibits GSK-3β activity and thus induces the β-catenin

pathway.[29,78] In order to study the role of curcumin in canonical Wnt pathway induction, NSC cultures were treated with the PI3K/Akt pathway inhibitor (LY294002) and the Wnt pathway inhibitor (Dkk-1) in the presence and absence of curcumin (Figure 9C). Both PI3K/Akt inhibitor and Wnt pathway inhibitor significantly reduced the phosphorylation of GSK-3β. We found curcumin enhanced the phosphorylation of GSK-3β even in PI3K/Akt inhibitor treated NSC cultures, suggesting curcumin can also enhance neurogenesis by a pathway other than activation of PI3K/Akt. Interestingly, phosphorylation of GSK-3β by curcumin was almost completely blocked in LY294002 and Dkk-1 co-treated cultures. These studies suggest that curcumin inhibits GSK-3β activity and thus increases neurogenesis through activation of the canonical Wnt-β-catenin pathway.

Genetic and Pharmacological Inhibition of the Wnt Pathway Reduces Curcumin-Induced Neurogenesis in the Hippocampus and NSC. Wnt3 plays an important role in the regulation of adult hippocampus neurogenesis through activation of the canonical Wnt pathway. We found curcumin enhanced the Wnt3 expression and protein levels, leading to enhanced neurogenesis by curcumin. We therefore investigated the specific involvement of the Wnt/β-catenin-mediated increased neurogenesis. Wnt3a was knocked down by stereotaxically injecting Wnt3a siRNA into the hippocampus, followed by treatment with bulk curcumin and curcumin nanoparticles. Neuronal differentiation was assessed by counting the number of BrdU/NeuN co-labeled cells (Figure 10A,B). Bulk curcumin and Cur-PLGA-NPs enhanced the number of BrdU/NeuN-positive neurons, which were significantly reduced by the Wnt3a siRNA. Neuronal differentiation promoting potential of curcumin nanoparticles was significantly inhibited by the Wnt3a siRNA (Figure 10A,B). Curcumin-mediated neuronal differentiation was also inhibited by the knockdown of Wnt3a in NSC cultures (Figure 10C,D). Further, in order to understand curcumin-mediated effects on the canonical Wnt-β-catenin pathway and neurogenesis, we have treated NSC with the Wnt pathway inhibitor Dkk-1 in the presence and absence of curcumin. We found that Dkk-1 protein reduced the number of β-tubulin-positive neurons in NSC culture. Treatment of Dkk-1 protein abolished neuronal differentiation enhancing potential of curcumin in the hippocampal-derived NSC culture (Figure 10E,F). These studies suggest a potential and specific role of the canonical Wnt pathway in curcumin-mediated induction of hippocampal neurogenesis.

Cur-PLGA-NPs Reverse Aβ-Mediated Inhibitory Effects on Hippocampal Neurogenesis and Learning and Memory in an AD Rat Model. Emerging evidence suggested that altered neurogenesis in the adult hippocampus plays an important role in pathogenesis of AD.[1,8,9] Hippocampal neurogenesis has functional implications and is critical for structural plasticity and maintenance of learning and memory processes throughout life.[1] Dysfunctional neurogenesis contributes to memory impairment as observed in AD.[8] Several key molecules that are involved in AD pathogenesis such as Aβ have been shown to reduce adult hippocampal neurogenesis.[8,79] Inhibition of the canonical Wnt pathway through interruption of the β-catenin signaling by Aβ leads to reduced neurogenesis in AD.[80] Loss of the Wnt signaling is implicated in the pathogenesis of AD.[36] Therefore, activation of the Wnt/β-catenin pathway, which leads to induction of neurogenesis, could be a promising therapeutic approach for improvement of learning and memory impairments in AD. We observed stimulatory effects of curcumin on hippocampal neurogenesis and activation of the Wnt pathway in our study. Thus we asked the question whether curcumin can reverse Aβ-mediated inhibitory effects on hippocampal neurogenesis and learning and memory defects in a rat model of AD-like phenotypes. We observed that intrahippocampal stereotaxic injection of Aβ significantly inhibited the proliferation of NSC (Figure 11A,B) and neuronal differentiation (Figure 11C,D). The numbers of BrdU$^+$ proliferating cells and β-tubulin$^+$ neurons were significantly decreased by the Aβ. A recent study suggested significantly decreased cell proliferation and neurogenesis in the hippocampus of Aβ-treated adult rats.[79] Cur-PLGA-NPs more significantly enhanced the number of BrdU$^+$ cells and neuronal differentiation and reduced Aβ-mediated inhibitory effects on neurogenesis as compared to bulk curcumin (Figure 11A−D). Empty PLGA-NPs did not produce any significant effects on the number of BrdU$^+$ cells and neuronal differentiation (data not shown). Similarly, Cur-PLGA-NPs also enhanced the number of BrdU/β-tubulin-positive neurons in the hippocampal-derived NSC cultures treated with Aβ (Supplementary Figure S7). As neurogenesis in the hippocampus regulates learning and memory, we assessed the cognitive functions followed by treatment of bulk curcumin and Cur-PLGA-NPs in an Aβ-induced rat model of AD-like phenotypes (Figure 11E). Aβ-mediated reduced neurogenesis resulted in significantly decreased learning and memory ability. We observed increased cognitive deficits in Aβ-treated rats as compared to control. Cur-PLGA-NPs produced a greater reversal of the Aβ-induced cognitive dysfunction in rats as compared to bulk curcumin (Figure 11E). Interestingly, we found that at a dose of 20 mg both bulk curcumin and curcumin nanoparticles significantly enhanced hippocampal neurogenesis and reversed Aβ-induced cognitive deficits. Bulk curcumin at a dose of 0.5 mg showed no significant enhancement of neurogenesis, while curcumin-loaded nanoparticles were effective at this dose also. These studies suggest that bulk curcumin is not able to enhance neurogenesis below a minimum threshold level, while curcumin nanoparticles may be effective even at much lower doses *in vivo*

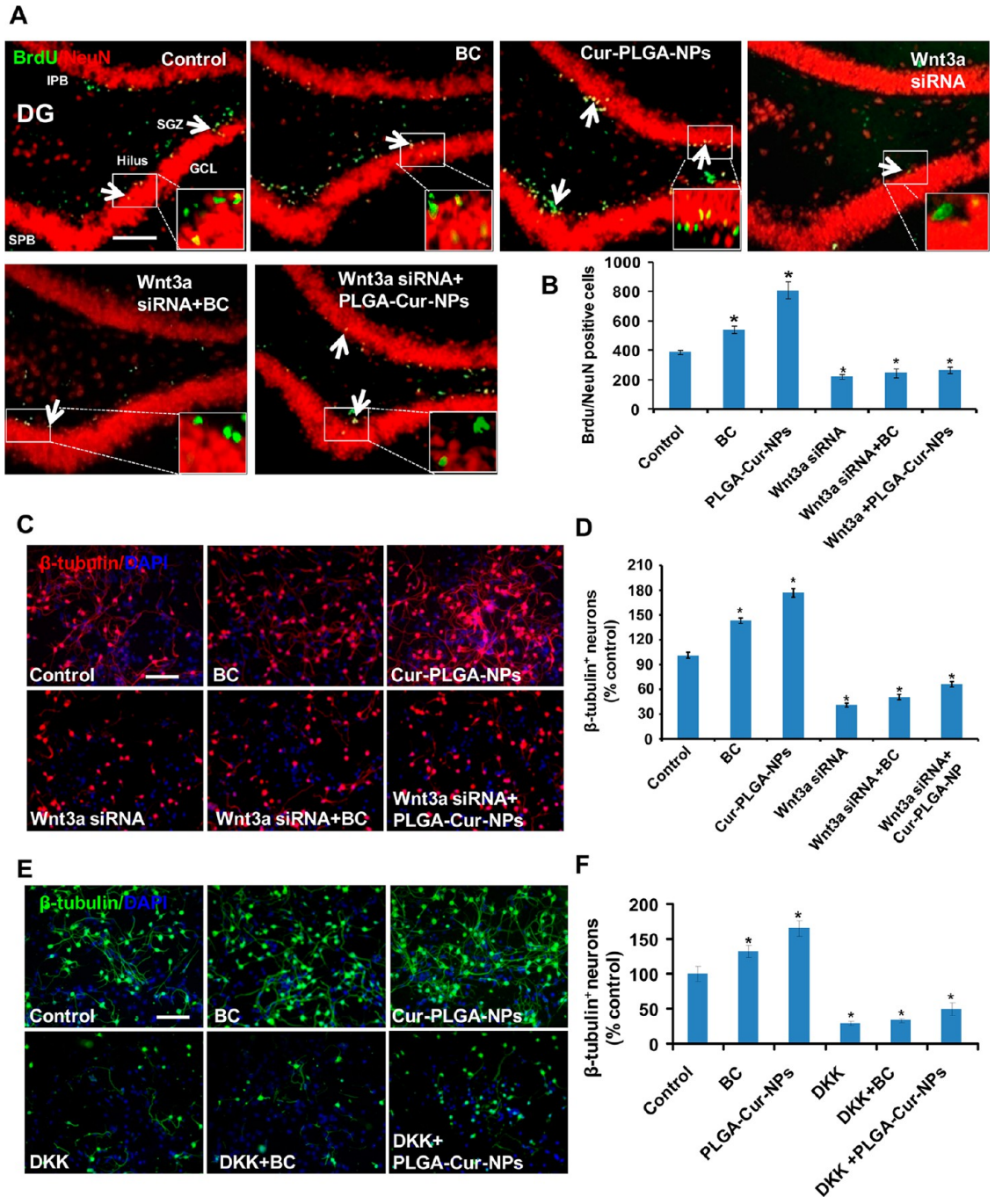

Figure 10. Pharmacological and genetic inhibition of the Wnt pathway reduces Cur-PLGA-NP-mediated stimulatory effects on neuronal differentiation in the hippocampus and NSC cultures. (A, B) Wnt3a knockdown was done by the stereotaxic injection of Wnt3a siRNA and scrambled sequences directly into the hippocampus of control, BC-, and Cur-PLGA-NP-treated rats. Wnt3 knockdown significantly reduced the number of BrdU/NeuN-positive neurons in the BC and Cur-PLGA-NPs groups. (C, D) NSC cultures were transiently transfected with Wnt3 siRNA. Mean + SEM of three independent experiments. *$p < 0.05$ *versus* control. Scale bar = 100 μm. (E, F) NSC cultures were treated with Wnt pathway inhibitor Dkk-1 and PI3K/Akt inhibitor LY294002 in the presence and absence of Cur-PLGA-NPs and bulk curcumin. Dkk-1 protein abolished neuronal differentiation enhancing potential of curcumin in the hippocampal-derived NSC culture. Values are expressed as mean ± SEM ($n = 4$). *$p < 0.05$ *versus* control.

(Figure 11A–E). We observed no significant effects on learning and memory in empty PLGA-NP-treated rats (data not shown). Cur-PLGA-NPs also inhibited Aβ-induced neurodegeneration in the hippocampus (Supplementary Figure S8). The number of Fluoro Jade-C$^+$ neurons was significantly decreased by Cur-PLGA-NPs in the hippocampus of Aβ-treated rats. These data are in accordance with earlier studies, where LiCl and rosiglitazone increased hippocampal neurogenesis and improved cognitive functions in AD transgenic mice by activation of the Wnt/β-catenin signaling.[81,82] A recent study found that curcumin-loaded

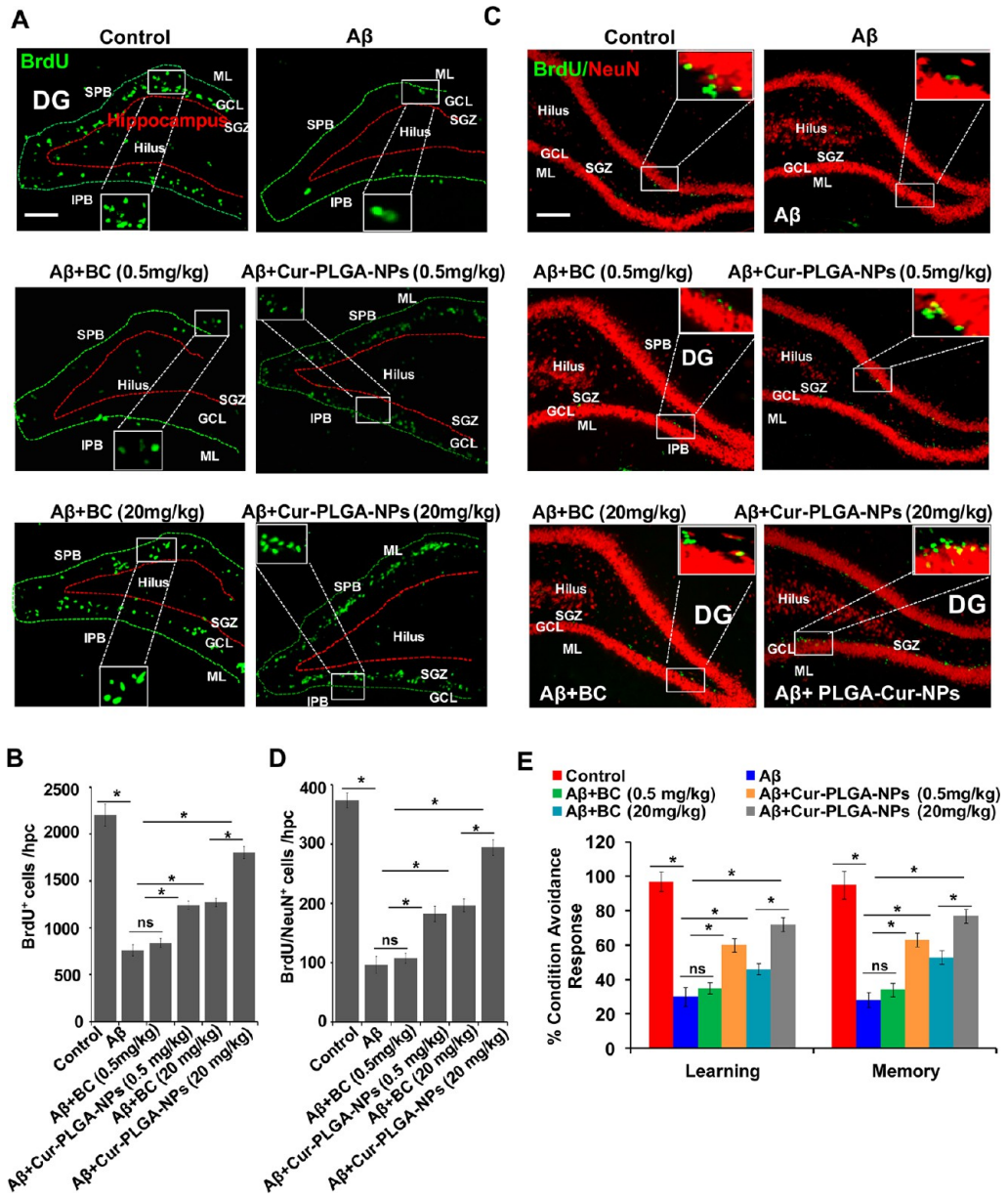

Figure 11. Cur-PLGA-NPs provide neuroprotection against Aβ-induced neurodegeneration and reverses learning and memory deficits. (A, B) Photomicrographs showing immunostaining of BrdU$^+$ cells in the dentate gyrus region of the hippocampus. Rats were given a single stereotaxic injection of Aβ in the hippocampus. After one week of Aβ injection, rats were treated with 0.5 and 20 mg/kg body weight BC and Cur-PLGA-NPs. DG = dentate gyrus, SGZ = subgranular zone, GCL = granular cell layer, ML = molecular layer. (D) Quantification of BrdU$^+$ cells in the hippocampus. Values are expressed as mean $\pm$ SEM (n = 6 rats/group), ns = nonsignificant. *p < 0.05. (C, D) Double immunofluorescence analysis of matured neurons co-labeled with β-tubulin (red: marker for mature neurons) and BrdU (green) in the dentate gyrus region of the hippocampus Scale bar = 20 μm. (B) The quantitative analysis of β-tubulin/BrdU co-labeled cells suggests that Cur-PLGA-NPs significantly enhanced the neuronal differentiation in the Cur-PLGA-NPs + Aβ group, which was inhibited by Aβ. Values are expressed as mean $\pm$ SEM (n = 3). *p < 0.05. (E) The cognitive ability (learning and memory) of the control and Aβ-, BC-, and Cur-PLGA-NPs+ Aβ-treated rats was measured following assessment of two-way conditioned avoidance behavior. Cur-PLGA-NPs significantly reversed the Aβ-induced deficits in learning and memory as compared to control rats. Values are expressed as mean $\pm$ SEM (n = 6 rats/group). *p < 0.05.

PLGA nanoparticles tagged with Tet1 caused degradation of Aβ.[83] Our data suggest that Cur-PLGA-NPs can improve Aβ-mediated reduced neurogenesis and cognitive deficits through induction of the Wnt/β-catenin signaling.

***In Silico* Prediction of Molecular Targets of Curcumin in the Wnt/β-Catenin Pathway; Curcumin Interacts with Wif-1, Dkk-1, and GSK-3β.** In the experimental settings, we found up-regulation in mRNA expression of Wnt, LRP-5/6, β-catenin, LEF, and cyclin-D1 and down-regulation of Wif-1, Dkk-1, and GSK-3β genes in Cur-PLGA-NP-treated rats. To investigate the molecular mechanism for the up-regulation of Wnt and other downstream genes in the Wnt signaling cascade, we performed

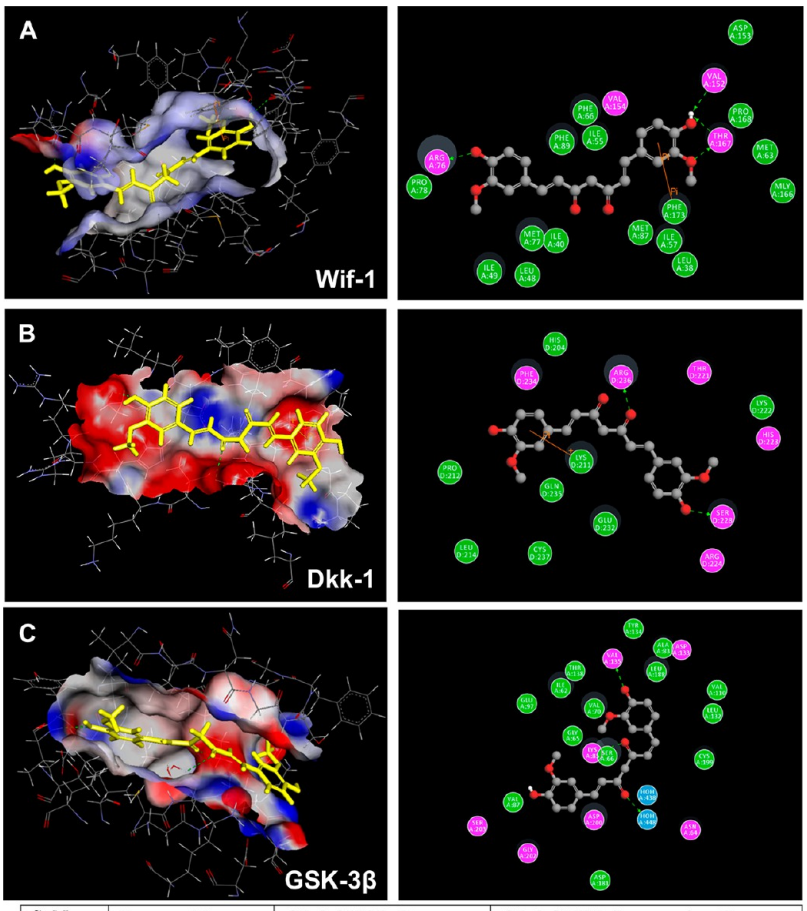

S. No.	Targets Name	CDOCKER Energy	CDOCKER Interaction Energy
1	Wif-1	-32.56 Kcal/mol	-44.52 Kcal/mol
2	Dkk-1	-26.47 Kcal/mol	-37.33 Kcal/mol
3	GSK-3β	-23.27 Kcal/mol	-36.49 Kcal/mol

Figure 12. ***In silico*** **molecular docking studies suggest several targets of curcumin in the Wnt/β-catenin pathway: Surface is generated around the curcumin (yellow color) in the binding cavity and colored by hydrogen bond character, with receptor donor colored in pink and receptor acceptor in green. A 2D depiction of curcumin and the binding site residues of (A) Wif-1, (B) Dkk-1, and (C) GSK-3β. Hydrogen bonds and pi interaction between the surrounding amino acid residues and the ligand are also displayed. Curcumin molecule is depicted in yellow color.**

detailed computational molecular docking studies with various key regulatory enzymes in the Wnt pathway. A set of 10 low-energy conformations of curcumin were generated using the "Generate conformation" protocol of DS3.5. The absolute energy of the lowest energy conformation of curcumin was −20.9748 kcal/mol. A total of eight rotatable bonds were present in the curcumin molecule, which are used to generate various conformations in the molecular docking studies. We found plausible binding modes of curcumin in the active site of Wif-1, Dkk-1, and GSK-3β (Figure 12A−C). However, no interaction of curcumin was observed in the functional site of sFRP, Wnt, Frizzled, LRP-5/6, Axin, APC, β-catenin, and TCF proteins, when analyzed with the CDOCKER protocol of Accelrys Discovery Studio 3.5 (data not shown).

Wif-1 directly interacts with Wnt protein and prevents the ternary complex with the cell surface receptors Frizzled and LRP-5/6, which is required for the downstream signal transduction and the activation of Wnt target genes.[84,85] The functional site of Wif-1 that interacts with Wnt was analyzed from its 3D structure available in the protein data bank (PDB ID: 2YGN). We defined a binding sphere with radius 12.5 Å around the Wif domain lipid-binding pocket. The best binding pose of the Wif-1 and curcumin complex has a CDOCKER energy of −32.56 kcal/mol and a CDOCKER interaction energy of −44.52 kcal/mol. These energy profiles suggest that curcumin might be a good inhibitor of Wif-1 that blocks the interaction sites for the Wnt protein. In the best binding pose, selected on the basis of CDOCKER energy, a total four hydrogen bonds were formed between curcumin and Arg76, Thr167, and Val152 amino acid residues in the binding site of Wif-1, and one pi−pi interaction was also observed with Phe173 present in the lipid-binding pocket of the

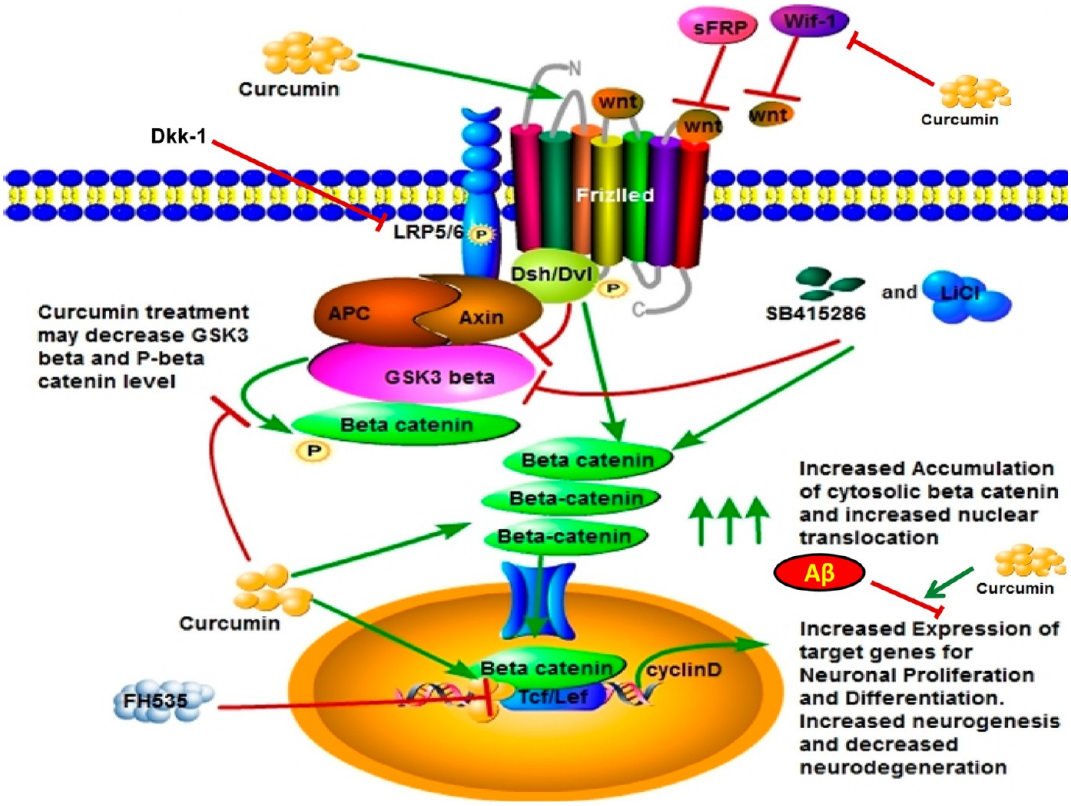

Figure 13. Proposed schematic model for the role of curcumin in neurogenesis through activation of the Wnt/β-catenin signaling pathway: On the basis of experimental and *in silico* studies we found that curcumin may increase Wnt levels by interacting with Wnt inhibitory molecules such as Wif-1 and Dkk-1, thus activating the Wnt pathway. Wnt interacts with the 7-transmembrane Frizzled receptor and phosphorylated co-receptor low-density lipoprotein (LRP-5/6), which triggers activation of cytoplasmic dishevelled (Dvl) protein. Activated Dvl then interacts with destruction complex Axin/APC/GSK-3β and inhibits GSK-3β, which phosphorylates β-catenin and promotes β-catenin degradation through proteasomal degradation in the absence of Wnt. Inhibition of GSK-3β leads to accumulation of cytoplasmic β-catenin and its translocation into the nucleus. In the nucleus β-catenin interacts with the TCF/LEF promoter complex, leading to activation of target genes that are involved in proliferation and differentiation of NSC. After cellular internalization curcumin may likely interact with GSK-3β, thus enhancing the levels of cytoplasmic β-catenin, and decrease its phosphorylation. Curcumin then enhances β-catenin nuclear translocation, leading to enhanced TCF/LEF and cyclin-D1 promoter activity and increased neurogenesis. The blockage of the Wnt/β-catenin signaling through Wnt siRNA, Dkk-1, and TCF inhibitor FH535 leads to inhibition of curcumin-mediated cell proliferation and neuronal differentiation. Curcumin also blocks Aβ-mediated inhibitory effects on neurogenesis through induction of the Wnt/β-catenin signaling.

receptor (Figure 12A). The curcumin interaction with the Wnt binding site of Wif-1 might be the reason for the increased expression and protein levels of Wnt in our study.

Dkk-1 is a secreted glycoprotein that binds with LRP-6 and inhibits the Wnt signaling by blocking Wnt-mediated Frizzled-LRP complex formation. In our study, we found up-regulation of Wnt, Frizzled, and LRP-5/6 mRNA expression with the exposure to curcumin. These findings motivated us to investigate if the up-regulation of the Wnt signaling cascade is mediated by the inhibition of Dkk-1 activity due to binding of curcumin to its LRP-5/6 binding domain. A binding sphere with a radius of ~13 Å was defined around the Dkk-1 and LRP-6 binding site from the 3D coordinate file obtained from the Protein Data Bank (PDB ID: 3S8 V). We observed the interaction of curcumin with the Ser228 and Arg236 amino acid residues of Dkk-1, which are involved in the hydrogen bond formation with the His834 and Asp811 residues of LRP-6, respectively (Figure 12B). Also, a cation$-\pi$ interaction was formed between Lys211 of Dkk-1 and one of the aromatic rings of curcumin. The CDOCKER energy and CDOCKER interaction energy for the curcumin interaction pose were -26.47 and -37.33 kcal/mol, respectively. These observations indicate that curcumin binding with Dkk-1 will interfere with Dkk-1-mediated inhibition of Wnt-Frizzled-LRP6 complex formation required to initiate the downstream signaling.

Recognizing the central role of GSK-3β in the Wnt signaling pathway, several GSK-3β inhibitors have been developed in the past for therapeutic purposes.[86] We also compared the binding efficiency of curcumin with the known GSK-3β inhibitor SB415286, which inhibits GSK-3β in an ATP competitive manner, using the CDOCKER protocol of DS3.5. Curcumin showed a high binding affinity with GSK-3β (CDOCKER energy -23.27 kcal/mol and CDOCKER interaction energy

−36.49 kcal/mol) in comparison to SB415286 (CDOCKER energy −9.21 kcal/mol) in the GSK-3β binding cavity. Figure 12C shows the curcumin in the functional site of GSK-3β. We explained that the increased expression of genes of the Wnt-Frizzled-LRP6 complex could be due to the curcumin interaction with Dkk-1, leading to activation of the Wnt pathway. Our study explained the increased expression and protein levels of Wnt due to curcumin's interaction with Wif-1, Dkk-1, and GSK-3β. As Wif-1 and Dkk-1 are negative regulators of the Wnt pathway, interaction of curcumin with Wif-1 and Dkk-1 may lead to increased expression and protein levels of Wnt3 and activation of the Wnt pathway. Further, GSK-3β is also a negative regulator of the Wnt pathway and causes phosphorylation of β-catenin; thus interaction of curcumin with GSK-3β may also lead to the activation of the Wnt pathway.

Cur-PLGA-NPs caused significantly decreased expression of Wif-1 and Dkk-1 as compared to bulk curcumin. Wif-1 is a protein that interacts with Wnt and inhibits the activation of the Wnt pathway. Similarly, Dkk is a negative regulator (antagonist) of the Wnt pathway and acts through inhibition of LRP-5/6, which is required for the activation of the Wnt pathway.

On the basis of our experimental and *in silico* studies, we proposed a schematic model illustrating the plausible mechanism(s) of curcumin-mediated alterations of NSC proliferation and differentiation through the Wnt/β-catenin signaling pathway (Figure 13). Curcumin possibly induces Wnt signaling by interaction with Wnt inhibitory molecules such as Wif-1 and Dkk-1, thus altering the expression of Wnt and its downstream target genes. After cellular internalization curcumin likely interacts with GSK-3β, thus enhancing the levels of cytoplasmic β-catenin, and decreases its phosphorylation. Curcumin then enhances β-catenin nuclear translocation, leading to enhanced TCF/LEF and cyclin-D1 promoter activity and increased neurogenesis. The blockage of the Wnt/β-catenin signaling through Wnt siRNA, Dkk-1 protein, or the TCF inhibitor FH535 leads to the inhibition of curcumin-mediated cell proliferation and neuronal differentiation. Curcumin also blocks Aβ-mediated inhibitory effects on neurogenesis through induction of Wnt/β-catenin signaling.

CONCLUSIONS

Herein, we report a novel method to increase adult neurogenesis through the use of a Cur-PLGA-NPs formulation. In conclusion, we found that Cur-PLGA-NPs potently induce NSC proliferation and neuronal differentiation *in vitro* and in the hippocampus and SVZ *in vivo*, as compared to bulk curcumin. Cur-PLGA-NPs internalize into the NSC in culture and also reach the brain. Curcumin nanoparticles enhance proliferation at very low dose and were not cytotoxic even at high doses as compared to bulk curcumin. Our study for the first time shows that curcumin increases reelin and Pax6 expression in the hippocampus. The expression of a panel of genes involved in NSC proliferation, self-renewal, and neuronal differentiation was significantly enhanced by Cur-PLGA-NPs. Interestingly, stereotaxic intrahippocampal administration of Cur-PLGA-NPs also enhanced neuronal differentiation. Curcumin nanoparticles increase neuronal differentiation by enhancing nuclear translocation of β-catenin and increasing phosphorylation of GSK-3β, which enhances expression of proneurogenic genes. Inhibition of the Wnt pathway through pharmacological inhibitors and siRNA blocked the neurogenesis-enhancing potential of curcumin. Cur-PLGA-NPs reverse Aβ-mediated inhibitory effects on hippocampal neurogenesis and learning and memory in an AD rat model. Molecular docking studies predict that curcumin may activate Wnt/β-catenin signaling and modulates neurogenesis through interaction with Wif-1, Dkk-1, and GSK-3β. Our results provide evidence that curcumin nanoparticles induce adult neurogenesis and may provide a novel therapeutic target for both regenerative medicine and for the treatment of neurodegenerative diseases.

MATERIALS AND METHODS

Materials. PLGA (average MW 25 kDa), curcumin, 3-[4,5-dimethylthiazol-2-yl]-2,5-diphenyltetrazolium bromide (MTT), Aβ, SB415286, agarose, Tris, tetramethylrhodamine isothiocyanate (TRITC), bromodeoxyuridine (BrdU), alamar blue, 4,6-diamidino-2-phenylindole dilactate (DAPI), basic fibroblast growth factor (bFGF), epidermal growth factor (EGF), serum-free neurobasal medium, N-2 supplement, B-27 supplement, fetal bovine/calf serum, Hank's balanced salt solution (HBSS), normal goat serum (NGS) antibiotic−antimycotic solution, and TRIzol reagent were obtained from Gibco BRL (Rockville, MD, USA). Bovine serum albumin (BSA), poly-L-lysine (PLL), bromophenol blue, rabbit anti-glial fibrillary acidic protein (GFAP) antibody, LY294002, and protease and phosphatase inhibitors were procured from Sigma Aldrich (USA). Recombinant human Dkk-1 protein and Lipofectamine LTX were procured from Invitrogen (Carlsbad, CA, USA). Cell culture products were purchased from Gibco-BRL-Life Technologies (UK). Monoclonal mouse anti-neuronal nuclei (NeuN) and nitrocellulose membrane were obtained from Chemicon (Millipore, Billerica, MA, USA). Mouse anti-β-actin, mouse anti-BrdU, rabbit anti-doublecortin (DCX), mouse anti-phospho-histone-H3, rabbit anti-GSK3-β, rabbit anti-p-GSK-3α/β, rabbit anti-β-catenin, rabbit anti-p-β-catenin, and rabbit anti-TCF/LEF primary antibodies were obtained from Cell Signaling Technology (Danvers, MA, USA). Rabbit anti-dishevelled primary antibody was obtained from Abcam (USA). Goat anti-Wnt3a was procured from Santa Cruz Biotechnology (Santa Cruz, CA, USA). Alexa Fluor 488 and Alexa Fluor 594 conjugated secondary antibodies were purchased from Molecular Probes (Invitrogen, USA). Primers were procured from Integrated DNA Technologies (IDT; Coralville, USA) and SYBR Green from Applied Biosystems (USA). Antifade mounting medium was obtained from Vector Laboratories (Vectashield, Vector Laboratories, CA, USA). Dual-Glo luciferase assay system

was purchased from Promega (USA). Culture wares were procured from Nunc (Roskilde, Denmark).

Preparation of Cur-PLGA-NPs. Cur-PLGA-NPs were prepared following the emulsion solvent evaporation method with slight modifications.[25] Briefly, 40 mg of curcumin was dissolved in 1 mL of acetone, PLGA (200 mg) solution prepared in 3 mL of DCM was added, and the mixture was stirred at 1600 rpm for 10 min. This mixture was added to a 1% PVA solution, stirred for 6 h for complete removal of organic solvent, followed by centrifugation at 12 000 rpm for 35 min at 4 °C. The pellet was resuspended in water and centrifuged again. This process was repeated several times. Finally nanoparticles were freeze-dried to obtain a solid dry powder. Nanoparticles were stored at 4 °C under anhydrous conditions for further studies.

Preparation of Fluorescein-Labeled PLGA Nanoparticles. Fluoresceinylated PLGA nanoparticles were prepared in a two-step reaction. In the first step, 1 mmol of t-Boc-protected ethylenediamine was dissolved in 5 mL of DMF, and 1.1 mmol of FITC was added. This mixture was stirred in the dark at room temperature for 12 h, followed by removal of the solvent. The residue was mixed in a solution of trifluoroacetic acid/dichloromethane (2 mL, 1:1, v/v) by shaking for 1 h. The reaction mixture was concentrated on a rotary evaporator to obtain a residual mass, triturated with 10 mL of dichloromethane, and dried under vacuum to obtain fluoresceinyl-ethylenediamine (F-EDA).

In the second step, fluoresceinyl-ethylenediamine was attached with PLGA. The 50 mg of PLGA was dissolved in 1 mL of DMF. To this mixture were added *N*-hydroxysuccinimide (1.5 μg), F-EDA (5 μg, for 1% substitution), EDAC (2.5 μg), and TEA (4 μL). The reaction mixture was stirred at room temperature for 6 h. The mixture was concentrated on a rotary evaporator, and the residue was partitioned between dichloromethane and water. The organic phase was collected and concentrated to dryness. The syrupy material was dissolved in 2 mL of dichloromethane and added dropwise into a solution of 1% PVA, and the mixture was stirred for 3 h at room temperature. The solution was centrifuged, and the pellet was washed three times with water and freeze-dried to obtain fluoresceinyl-PLGA nanoparticles.

Characteristics of Cur-PLGA-NPs. *Size and Zeta-Potential Measurements.* The zeta-potential and mean particle size of Cur-PLGA-NPs were measured by dynamic laser light scattering using a Zetasizer Nano-ZS (Malvern Instruments, U.K). The nanoparticles were suspended in water at a concentration of 1 mg/mL. The mean particles' size and charge were measured at 25 ± 2 °C, by following settings in the Zetasizer: nominal 5 mW He−Ne laser operating at 633 nm wavelength; viscosity for water 0.89 cP, and refractive index of water 1.33. Zeta-potential values were presented as an average value of 30 runs, and the Smoluchowski approximation was used to calculate the zeta-potential from the electrophoretic mobility.[87]

Encapsulation Efficiency. The encapsulation efficiency of curcumin was determined by the spectrophotometric method. Briefly, 10 mg of curcumin nanoparticles was dissolved in 2 mL of DCM and kept in an incubator shaker (Heidolph Instruments) with stirring for 30 min. The absorbance of the solution was measured at 427 nm. The amount of encapsulated curcumin was calculated from the standard curve drawn between varied amount of curcumin and absorbance, and all the measurements were carried out in triplicate. The encapsulation efficiency (EE) was determined from the following formula.

$$\mathrm{EE}\% = \frac{\text{weight of curcumin in nanoparticles}}{\text{weight of curcumin used for nanoparticle preparation}} \times 100$$

In Vitro Drug Release Study. Cur-PLGA-NPs were evaluated for *in vitro* curcumin release kinetics by the dialysis method, as previously reported.[88] Curcumin nanoparticles (10 mg) were dispersed in a 50% ethanol solution (1 mL), and the solution was transferred to a dialysis bag (12 kDa cut off) and allowed to dialyze against 60 mL of 50% ethanol with constant stirring at 50 rpm in an incubator shaker at 37 ± 2 °C. At predetermined time intervals, an aliquot (1 mL) of the sample was withdrawn, its absorbance was measured at 427 nm, and the same amount of fresh medium was added to the dialysis container. The amount of the released curcumin was calculated using a standard curve of pure curcumin in the same solvent.

Primary Culture of Hippocampal NSC. Pregnant Wistar rats were deeply anaesthetized with a ketamine and xylazine mixture. The hippocampus contains a pool of NSC, which readily form neurospheres in culture. A neurosphere is an aggregate of several multipotent and self-renewing NSC, which can differentiate into neurons, glial cells, and oligodendrocytes. Briefly, hippocampal tissue was dissected from embryonic day-12 rat embryos, washed with cold HBSS, and chopped with a surgical blade into small pieces. The pieces were then transferred into tubes containing 0.05% trypsin/EDTA at 37 °C for 30 min followed by addition of 0.5 mg/mL trypsin soybean inhibitor. A single-cell suspension was prepared by gentle trituration. Cells were resuspended in neurobasal medium containing 2 mM L-glutamine, 1% antibiotic−antimycotic, 2% B-27, 1% N-2 supplement, and 20 ng/mL each of EGF and bFGF. Flasks containing cells were placed in a humidified CO_2 incubator at 37 °C with 5% CO_2. Neurosphere formation occurs after 5−7 days.

In Vitro Curcumin Cellular Uptake Study. Flow cytometry was carried out to study the cellular uptake of FITC-tagged Cur-PLGA-NPs (FITC-Cur-PLGA-NPs) following an earlier published method.[83] In brief, hippocampus-derived NSC were treated with FITC-Cur-PLGA-NPs and empty PLGA-NPs for 6 h. Cells were then washed twice with PBS to remove unbound FITC-Cur-PLGA-NPs followed by trypsinization and resuspension in 500 μL of PBS. Cells were fixed with 4% paraformaldehyde for 20 min, washed three times with PBS, and permeabilized with 500 μL of ice-cold methanol for 10 min. Cells were washed again with PBS and resuspended in 500 μL of PBS. Flow cytometry analysis was carried out using the FITC channel. Results were expressed in terms of mean fluorescence intensity of FITC.

MTT and Alamar Blue Reduction Assay for Cell Viability and Proliferation. To examine the effects of bulk curcumin and Cur-PLGA-NPs on NSC proliferation in culture, the MTT assay and alamar blue reduction assay were carried out. In brief, NSC were plated in a 96-well plate at a density of 1×10^4 cells/well. Cultures were treated with different concentrations of bulk curcumin and Cur-PLGA-NPs (0.1, 0.2, 0.5, 5, and 50 μM) for 24 h. The MTT assay was carried out following an earlier published method.[89]

NSC proliferation/viability were measured using the alamar blue reduction assay. This assay is based on resazurin reduction due to metabolic activity of the living cells. After respective treatments, cultures were incubated in alamar blue reagent for 4 h at 37 °C. Vehicle-treated cells served as a control. Background florescence was measured by adding 10 μL of alamar blue solution/well in medium having no cells. Alamar blue dye reduction in terms of fluorescence intensity was measured at 530 nm excitation and 590 nm emission in a Synergy HT microplate reader (BIO-TEK, Germany) with KC4 software (Germany). Values of background florescence were subtracted from the experimental values. Experiments were performed in triplicates, and relative cell viability was calculated using the following formula:

$$\text{relative cell proliferation} = [\text{absorbance}_{\text{sample}}/\text{absorbance}_{\text{control}}] \times 100$$

Results were expressed in terms of alamar blue reduction % of control.

Neurosphere Growth Kinetics Assay. In order to assess the effects of Cur-PLGA-NPs on cell proliferation and neurosphere formation, the neurosphere growth kinetics assay was performed as described earlier.[90] In brief, a hippocampal single-cell suspension was plated in a 12-well plate at a density of 50 000 cells/well in neurobasal medium containing B-27, N-2, bFGF, and EGF. Cultures were treated with bulk curcumin, empty PLGA-NPs, and Cur-PLGA-NPs. The number and size of neurospheres were analyzed in all the groups using a Nikon Eclipse Ti-S inverted fluorescent microscope equipped with a Nikon Digital Sight Ds-Ri1 CCD camera and NIS Elements BR imaging software (Nikon, Japan).

Animals and Curcumin Treatment. The Wistar rats were obtained from Animal Breeding Colony of the Indian Institute of Toxicology Research and were kept in a 12 h light/dark cycle with *ad libitum* water and pellet diet (Hindustan Lever Laboratory

Animal Feed, India). Experimental animals were handled according to the guidelines laid down by the Institutional Ethical Committee for the animal experiments. Animals were randomly segregated into the following groups. The detailed experimental design is shown in Supplementary Figure S1.

Vehicle Control Group. Received daily single intraperitoneal (ip) injection of vehicle, 0.9% normal saline, for three weeks from PND28 to PND49.

Empty PLGA-NP-Treated Group. Received daily single ip injection of empty PLGA-NPs in normal saline from PND28 to PND49.

Bulk Curcumin-Treated Group. Received daily single ip injection of bulk curcumin (5, 10, and 20 mg/kg body weight) from PND28 to PND49.

Cur-PLGA-NPs-Treated Group. Received daily single ip injection of Cur-PLGA-NPs (5, 10, and 20 mg/kg body weight) from PND28 to PND49.

After respective treatments at PND49, rats were subjected to neurochemical and immunohistochemical studies. To determine the effects of curcumin on NSC proliferation, rats from different groups were sacrificed 4 h after the last BrdU injection at PND49. Further, to evaluate the effects of curcumin on NSC survival/differentiation or cell phenotype, rats of another set were allowed to live for an additional 3 weeks after the last BrdU injection.[90] Animals were sacrificed at PND70 for double immunofluorescence analysis of BrdU and neuronal or glial markers as described earlier[90] (Supplementary Figure S1).

Levels of Curcumin Analysis by HPLC. Levels of curcumin in the hippocampus of rats treated with bulk curcumin and Cur-PLGA-NPs were measured using a Waters 515 HPLC system (USA) following an earlier published method.[91] Briefly, the hippocampus was dissected, weighed, and homogenized in 1 mL of chilled PBS. Extraction buffer (95% ethyl acetate and 5% methanol v/v) was added in each sample followed by vortexing and centrifugation at 12 000 rpm for 10 min at 4 °C. Supernatants were collected and dried using N_2 gas. Dried samples were resuspended in a mobile phase (49% acetonitrile, 20% methanol, 30% deionized H_2O, and 1% acetic acid). Extract was separated by a PDA detector at 420 nm with a flow rate of 1.5 mL/min for 10 min. The stock solutions of bulk curcumin and Cur-PLGA-NPs were diluted to appropriate concentrations for construction of calibration curves by plotting the mean peak areas *versus* the concentration of standards. Results are expressed in terms of curcumin concentration (μg/g wet tissue).

Intracellular Localization of Cur-PLGA-NPs in the Hippocampus and NSC Culture. Ultracellular localization of Cur-PLGA-NPs in the brain and NSC culture was assessed using TEM. Brain was removed after transcardial perfusion with 4% PFA, and the hippocampus was dissected and cut into small pieces (2 mm). These pieces were fixed with 2.5% glutaraldehyde at 4 °C overnight, followed by postfixation with osmium tetraoxide (OsO_4) for 2 h at room temperature. Similarly, a pellet of NSC was fixed with a mixture of 2.5% glutaraldehyde for 1 h at 37 °C, rinsed with sodium cacodylate buffer, and postfixed in 1% aqueous OsO_4 for 1 h at room temperature. After removal of OsO_4, the pieces/pellet were dehydrated in graded acetone (10−100%). The pieces/pellet were then rehydrated in propylene oxide, embedded in an Araldite and dodecenyl succinic anhydride mixture, and baked for 48 h at 65 °C. Ultrathin sections (50−70 nm) were cut with a Leica EM UC7 ultramicrotome, stained with uranyl acetate and lead citrate, and examined under TEM (FEI, Technai G2 Spirit TWIN, USA).

Internalization of FITC-Cur-PLGA-NPs in the Brain and NSC Cultures. Localization of FITC-Cur-PLGA-NPs in the brain and NSC cultures was carried out by immunofluorescent detection of FITC nanoparticles under the FITC channel in an inverted fluorescence microscope.

BrdU Administration for Immunohistochemical Analysis of Cell Fate and Proliferation in the Hippocampus and SVZ. After respective treatments, rats received a daily single ip injection of BrdU (50 mg/kg body weight) for five consecutive days from PND45 to PND49. To determine the effects of curcumin on NSC proliferation, rats from control and curcumin-treated groups were sacrificed 4 h after the last BrdU injection at PND49. Brains were dissected for immunohistochemical detection of proliferating and newborn cells. Animals were sacrificed by transcardial perfusion under sodium pentobarbital deep anesthesia at PND49 for double immunofluorescence analysis of BrdU and neuronal or glial markers following an earlier published method.[90] Animals from each group were perfused with PBS (0.1 M, pH 7.2), followed by fixing with 4% ice-cold paraformaldehyde. Brains were removed and cryopreserved in 10%, 20%, and 30% (w/v) sucrose in PBS. Then 30 μm thin serial coronal sections encompassing the hippocampus and SVZ were cut using a freezing microtome (Slee Mainz Co., Germany). For immunohistochemical analysis of proliferating cells, every sixth section was taken, and sections were 180 μm apart from each other. Sections were treated with 2 N HCl for 30 min at 37 °C to denature the DNA, followed by neutralization with borate buffer (0.1 M, pH 8.5) for 10 min at room temperature. Sections were incubated in 0.5% H_2O_2 in methanol followed by blocking in 3% NGS, 0.5% BSA, and 0.1% Triton X-100. Sections were incubated for 24 h with primary monoclonal mouse anti-BrdU antibody (1:500) at 4 °C followed by incubation in Alexa Fluor-488 linked secondary antibody (1:200) for 2 h at room temperature. Slides were analyzed under a Nikon Eclipse Ti-S inverted fluorescent microscope.

Double Co-immunofluorescence Analysis in the Brain and NSC Cultures. In order to examine the effects of Cur-PLGA-NPs on neuronal and glial differentiation and cell phenotype of $BrdU^+$ proliferating cells, double immunofluorescence analysis was carried out in the hippocampus and SVZ at PND70 and NSC cultures following our earlier published method.[90] Coronal sections beginning at bregma −3.14 to −5.20 mm through the dorsal hippocampus encompassing the dentate gyrus region and 0.70 to −0.80 mm through the SVZ were co-labeled with BrdU/DCX (immature neuron marker), BrdU/NeuN or β-tubulin (mature neuron marker), and BrdU/GFAP (glial cell marker). Free-floating sections/NSC cultures were denatured with 2 N HCl and blocked with 3% NGS, 0.1% Triton X-100, and 0.5% BSA for 2 h. Sections were then incubated in mouse anti-BrdU (1:500), rabbit anti-DCX (1:200), rat anti-NeuN (1:500), and rabbit anti-GFAP (1:100) for 24 h at 4 °C. Additional sections were incubated with rabbit anti-GSK3β (1:100), rabbit anti-p-GSK3β (1:200), rabbit anti-β-catenin (1:200), rabbit anti-p-β-catenin (1:200), and mouse anti-phospho-histone-H3 primary antibodies (1:500). Secondary antibodies used were anti-mouse and anti-rabbit Alexa Fluor 488 (1:200) and anti-rabbit, anti-mouse, and anti-rat Alexa Fluor 594 (1:200). Sections were mounted with DAPI containing Hard Set antifade mounting medium (Vectashield, Vector Laboratories, CA, USA) and stored in the dark at 4 °C. Slides/cultures were analyzed for fluorescence co-labeling under a Nikon Eclipse Ti-S inverted fluorescent microscope equipped with a Nikon Digital Sight Ds-Ri1 CCD camera and NIS Elements BR imaging software (Nikon, Japan).

Immunocytochemistry. In order to assess the effects of Cur-PLGA-NPs on NSC proliferation and differentiation, immunocytochemistry was carried out. In brief, NSC were plated in chamber slides and treated with bulk curcumin, Cur-PLGA-NPs, β-catenin/TCF inhibitor FH535, GSK-3β inhibitors SB-415286 and LiCl, and Wnt3a protein. After respective treatments cells were fixed with 4% paraformaldehyde for 20 min. After washing, cells were incubated in blocking buffer (3% BSA and 0.1% Triton-X100) for 2 h at room temperature. Cells were incubated overnight at 4 °C with primary antibodies mouse monoclonal anti-Tuj1 (1:100), mouse anti-NeuN (1:100), and rabbit anti-GFAP (1:100). Cells were then incubated with Alexa Fluor conjugated secondary antibodies. Cells were stained with DAPI for nuclear labeling and mounted in DAPI containing antifade mounting medium. Fluorescent images were acquired using an inverted fluorescent microscope (Nikon).

Cell Quantification. Quantification of proliferating and differentiating cells was carried out following the earlier published studies.[90,92,93] In brief, an unbiased cell quantification method was used, where a person blind to the experimental groups carried out quantification in the SVZ and SGZ of the dentate gyrus. The dorsal hippocampus (dentate gyrus region) and the SVZ were identified at low magnification (10×), and a contour was drawn. Fluorescent-labeled cells were counted in every sixth section apart by at least 180 μm in 1/6 series, with a total of

six sections per rat analyzed as described earlier.[90,92,93] This spacing between two adjacent sections ensures that the same neuron will not be counted in two sections. To distinguish single cells within a cluster, cells were counted at higher magnification (600×), omitting cells in the outermost focal plane to avoid counting cell caps. A cell was counted in the SGZ of the dentate gyrus if it was in the SGZ or was touching it. Cells that were located at least two cell bodies away from the SGZ were considered located in the hilus region. Fluorescent images were captured for individual phenotype markers into green, red, and blue channels. Paired red and green fluorescent images were superimposed to form color-merged overlay images using NIS Elements BR imaging software. $BrdU^+$, phospho-histone-$H3^+$, β-$catenin^+$, p-GSK-$3\beta^+$, p-β-$catenin^+$, and DCX^+ cells were counted in sections through the hippocampus and SVZ of each rat brain. $BrdU^+$ cells were counted for BrdU/NeuN, BrdU/GFAP, BrdU/DCX, and BrdU/β-catenin co-labeling at a magnification of 600× in the dentate gyrus and SVZ. The number of labeled cells was determined by bilaterally counting labeled cells in six total sections and averaged for each rat. The total number of $BrdU^+$ cells in the hippocampus and SVZ was estimated by multiplying the total number of $BrdU^+$ cells from six sections by the section periodicity, *i.e.*, 6, and reported as the total number of $BrdU^+$ cells per rat. The data were expressed as the number of $BrdU^+$ cells co-labeled with phenotype marker.

Gene Expression Analysis by qRT-PCR. In order to measure the expression of genes involved in neurogenesis and the Wnt/β-catenin pathway, qRT-PCR analysis was carried out. In brief, total RNA was isolated from the hippocampus of control and treated rats/cultures using the TriZol reagent. Genomic DNA was removed using RNase free DNase (Ambion, USA). RNA pellets were resuspended in DEPC-treated water (Ambion). Equal amounts of RNA were reverse transcribed using the Superscript first-strand cDNA synthesis kit with Oligo-dT (Invitrogen, USA) and diluted in nuclease-free water (Ambion) to a final concentration of 10 ng/μL. Expression of cellular house-keeping gene β-actin served as a control to normalize values. Targets were detected and quantified in real time using the ABI Prism 7900 sequence detector system (PE Applied Biosystems; Foster City, CA, USA) and SYBR green chemistry (Applied Biosystems, USA). Relative expression was calculated using the $\Delta\Delta$Ct method. The sequences for primers are listed in the Supporting Information (Table S1).

Levels of Protein Analysis by Western Blot. The hippocampi of control and treated rats were homogenized in tissue homogenization buffer supplemented with protease and phosphatase inhibitors. Equal amounts of protein (45 μg) were loaded on 10% Tris-glycine gel. Membranes were blocked for 1 h at room temperature in Tris-buffered saline/Tween-20 (TBST) containing 5% nonfat dried milk. Membranes were incubated overnight at 4 °C with Wnt3 (1:1000), Wif-1 (1:5000), dishevelled (1:500), GSK-3β (1:1000), p-GSK-3β (1:500), TCF (1:1000), LRP-5/6 (1:1000), p-LRP-5/6 (1:1000), β-catenin (1:1000), p-β-catenin (1:1000), and β-actin (1:10 000). Membranes were then washed three times with TBST and incubated for 2 h with horseradish peroxidase-conjugated secondary antibody. Immunoreactive proteins were detected using a chemiluminescent substrate (Pierce, USA) according to the manufacturer's instructions. Protein bands were quantified using Scion Image for Windows (NIH, USA).

TCF/LEF and Cyclin-D1 Luciferase Reporter Assay. NSC were plated in 24-well plates at a density of 2×10^5 cells/well and treated with FH535, SB-415286, LiCl, and Wnt3a protein with and without curcumin. After exposure NSC were transiently transfected with the TCF/LEF and cyclin-D1 luciferase reporter plasmids using Lipofectamine reagent (Invitrogen). Luciferase activity was determined using a dual luciferase assay as per the manufacturer's instructions (Promega, USA).

Wnt3a Knockdown. Wnt3a knockdown was carried out by stereotaxic injection of Wnt3a siRNA directly into the hippocampus. Knockdown was done with a pool of target-specific siRNA sequences for Wnt3a and scrambled sequences. After knockdown, animals were treated with Cur-PLGA-NPs and bulk curcumin, and effects on neuronal differentiation were assessed using immunohistochemistry.

Wnt3a knockdown in NSC culture was carried out by transient transfection with Wnt3a siRNA and scrambled sequences. Transient transfection was performed with 10 nM Wnt3a siRNA at a cell confluence of approximately 70% using Lipofectamine LTX transfection reagent as per the manufacturer's protocol. After knockdown, the effect on NSC neuronal differentiation was assessed using immunocytochemistry and qRT-PCR.

Treatment of NSC with Canonical Wnt Pathway Inhibitor and PI3K/Akt Inhibitor. To assess the specific involvement of curcumin-mediated activation of the canonical Wnt pathway in neuronal differentiation, hippocampus-derived NSC cultures were treated with potent Wnt antagonist recombinant human protein Dkk-1 (100 nM) with and without Cur-PLGA-NPs and bulk curcumin. After respective treatments neuronal differentiation was assessed by immunocytochemistry.

Similarly, the specific role of Cur-PLGA-NP-mediated activation of the Wnt pathway in neurogenesis was assessed by treating NSC with Wnt pathway inhibitor Dkk-1 and PI3K/Akt inhibitor LY294002 in the presence and absence of Cur-PLGA-NPs and bulk curcumin. After treatment, immunoblotting was performed to study protein levels of GSK-3α/β and p-GSK-3α/β, a negative regulator of the canonical Wnt pathway.

Preparation of Aβ-Induced Rat Model of AD. Rats were anesthetized with ip injection of ketamine (100 mg/kg body weight) and xylazine (30 mg/kg body weight). PND28 rats were fixed in a stereotaxic apparatus (Stoelting Co., USA) and given a stereotaxic injection of 2 μL of Aβ (1−42) (0.2 μg/μL in saline) into both sides of the hippocampus, using a 10 μL Hamilton syringe at the following coordinates: AP −3.3, ML 2.0, DV 4.0 (in mm with respect to bregma). The injection rate was maintained at 1 μL/min using an autoinjector pump attached to the stereotaxic apparatus, and the cannula was left in place for 5 min and thereafter slowly retracted. After one week, at PND35, Aβ-injected rats were treated with bulk curcumin and Cur-PLGA-NPs daily for two consecutive weeks as per the following experimental plan (Supplementary Figure S1).

Experimental groups:

1. Group I (sham): received 2 μL of normal saline as vehicle
2. Group II: stereotaxic intrahippocampal injection of Aβ dissolved in normal saline
3. Group III: Aβ + empty PLGA-NPs
4. Group IV: Aβ + bulk curcumin (0.5 mg/kg body weight ip)
5. Group V: Aβ + Cur-PLGA-NPs (0.5 mg/kg body weight ip)
6. Group VI: Aβ + bulk curcumin (20 mg/kg body weight ip)
7. Group VII: Aβ + Cur-PLGA-NPs (20 mg/kg body weight ip)

A set of rats was sacrificed at PND49 for immunohistochemical cell proliferation study, while another at PND70 for cell survival/neuronal differentiation study in the dentate gyrus region and SVZ.

Fluoro-Jade C Labeling and Quantification. To monitor the neuroprotective potential of bulk curcumin and Cur-PLGA-NPs against Aβ-induced neurotoxicity, Fluoro-Jade C staining was used, which is an established detection technique for degenerating neurons.[94] Sections mounted on slides were air-dried at room temperature for 30 min and sequentially rehydrated in 1% NaOH in 80% ethanol for 5 min, 70% ethanol for 2 min, and distilled water for 2 min. The 0.06% potassium permanganate solution was applied onto the sections for 10 min followed by washing three times with distilled water. The sections were then immersed in 0.0004% Fluoro-Jade C solution in the dark for 30 min. Slides were washed three times in distilled water, dried at 50 °C, cleared in xylene, mounted in DAPI mounting medium, and observed under a fluorescence microscope.

Fluoro-Jade C^+ degenerating neurons in both hippocampi were counted as described earlier.[90] In brief, Fluoro-Jade C^+ neurons were counted in a total of six sections and averaged for each rat. The total number of Fluoro-Jade C^+ neurons in the hippocampus was calculated by multiplying the total number of Fluoro-Jade C^+ neurons in six sections by the section periodicity

(which is 6) and reported as the total number of Fluoro-Jade C^+ neurons/rat.

Conditioned Avoidance Response (CAR). The learning and memory ability of the control and curcumin-treated rats was measured following assessment of two-way conditioned avoidance response behavior in a shuttle box (Columbus Instruments) as published earlier.[90] In brief, rats from the control and treated groups were individually placed in one of the chambers in a shuttle box. Animals were given 20 trials/day repeatedly for consecutive days, until 90% CAR in the control group was achieved. On a given day, when learning or retention ability in rats of the control group reached ≥90% CAR, a comparison was made with the corresponding treated groups of the same day. The percentage of CAR was considered as a measure of cognitive ability between the control and treated group for analysis of learning and memory. To assess memory ability of the animals, rats were left for 7 days and CAR was measured in all the groups. Learning and memory in treated rats was calculated as compared to % of control.

***In Silico* Target Prediction Studies.** *Preparation of Ligands.* In order to investigate the molecular mechanism of curcumin-mediated Wnt signaling cascade regulation, we performed molecular docking studies with key regulatory enzymes of the Wnt signaling pathway using CDOCKER module of version 3.5 Discovery Studio molecular simulation package (Accelrys, San Diego, CA, USA).

The minimum energy conformation of the curcumin molecule (CID: 969516) was generated using the "Generate Conformations" protocol of Discovery Studio 3.5. Conformation method "FAST" was chosen to obtain 10 diverse low-energy conformations with the relative energy threshold of 20 kcal/mol. These low-energy conformations were further minimized using Smart Minimizer protocol for 200 steps by applying the CHARMm force field.

Preparation of Protein Structures. The initial 3D structures of probable receptors for curcumin in the Wnt signaling pathway such as Wif-1, SFRP, Wnt, Frizzled, Dkk-1, LRP-5/6, GSK-3β, Axin, APC, ICAT, β-catenin, and TCF were taken from the Protein Data Bank with the PDB ID 2YGN, 1IJX, 4F0A, 3S2K, 3I4B, 1QZ7, 3AU3, 1LUJ, and 1JPW, respectively. For all the probable receptors, nonstandard amino acid names and alternate conformations were removed and all the incomplete residues and terminal residues were modified. The CHARMm force field along with Momany Rone partial charges were applied on all the receptor molecules. Functional sites of respective proteins involved in the Wnt signaling cascade were identified on the basis of available experimental information from the public domain.

Molecular Docking Experiments. Docking studies were performed using the CDOCKER module, which is a grid-based molecular docking method that employs the CHARMm force field using a rigid receptor. A set of 10 starting random orientations of curcumin was produced by translating its center in the receptor active site through 1000 steps (1 fs/step) of high-temperature molecular dynamics (MD) with dynamic target temperature 1000 K. Electrostatic interactions were also included in the initial random structure generation. For each MD-generated ligand conformation, 10 rigid-body rotations about its center of mass were used as the initial conformations in the binding cavity. Further, simulated annealing (SA) was used to search low-energy conformations of the ligand in the binding pocket by heating for 2000 steps (1 fs/step) from a temperature of 300 K to 700 K followed by cooling back from 700 K to 300 K in 5000 steps (1 fs/step). The CHARMm force field was then used for final minimization of the ligand in the rigid receptor cavity. For each of the final poses, CHARMm energy and interaction energy were calculated. The poses were sorted by CHARMm energy, and the top scoring poses were retained for the analysis of curcumin binding mode with the receptors from the Wnt signaling pathway.

Statistical Analysis. Statistical analysis was carried out by using GraphPad InStat statistical analysis software (SanDiego, CA, USA). Homogeneity of variance between all the experimental groups was ascertained, and mean significant difference in the experimental groups was determined using one-way analysis of variance (ANOVA) followed by the Tukey−Kramer *post hoc* multiple comparisons test. *p*-Values of 0.05 were considered to be statistically significant.

Conflict of Interest: The authors declare no competing financial interest.

Acknowledgment. This work was supported by the Council of Scientific and Industrial Research (CSIR) Network grants MEDCHEM (BSC0108) and UNDO (BSC0103) to R.K.C. S.A. and B.S. are recipients of Junior Research Fellowships from CSIR, New Delhi. S.K.T. and A.Y. are recipients of a Senior Research Fellowship and a Junior Research Fellowship, respectively, from University Grants Commission, New Delhi. CSIR-IITR Manuscript Communication number 3169.

Supporting Information Available: Ten supplementary figures and a table. This material is available free of charge *via* the Internet at http://pubs.acs.org.

REFERENCES AND NOTES

1. Zhao, C.; Deng, W.; Gage, F. H. Mechanisms and Functional Implications of Adult Neurogenesis. *Cell* **2008**, *132*, 645–660.
2. Ming, G. L.; Song, H. Adult Neurogenesis in the Mammalian Central Nervous System. *Annu. Rev. Neurosci.* **2005**, *28*, 223–250.
3. van Praag, H.; Schinder, A. F.; Christie, B. R.; Toni, N.; Palmer, T. D.; Gage, F. H. Functional Neurogenesis in the Adult Hippocampus. *Nature* **2002**, *415*, 1030–1034.
4. Clelland, C. D.; Choi, M.; Romberg, C.; Clemenson, G. D., Jr.; Fragniere, A.; Tyers, P.; Jessberger, S.; Saksida, L. M.; Barker, R. A.; Gage, F. H.; *et al.* A Functional Role for Adult Hippocampal Neurogenesis in Spatial Pattern Separation. *Science* **2009**, *325*, 210–213.
5. Marxreiter, F.; Regensburger, M.; Winkler, J. Adult Neurogenesis in Parkinson's Disease. *Cell. Mol. Life Sci.* **2013**, *70*, 459–473.
6. Lazarov, O.; Mattson, M. P.; Peterson, D. A.; Pimplikar, S. W.; van Praag, H. When Neurogenesis Encounters Aging and Disease. *Trends Neurosci.* **2010**, *33*, 569–579.
7. Winner, B.; Kohl, Z.; Gage, F. H. Neurodegenerative Disease and Adult Neurogenesis. *Eur. J. Neurosci.* **2013**, *33*, 1139–1151.
8. Mu, Y.; Gage, F. H. Adult Hippocampal Neurogenesis and Its Role in Alzheimer's Disease. *Mol. Neurodegener.* **2011**, *6*, 85.
9. Steiner, B.; Wolf, S.; Kempermann, G. Adult Neurogenesis and Neurodegenerative Disease. *Regener. Med.* **2006**, *1*, 15–28.
10. Cho, S. R.; Benraiss, A.; Chmielnicki, E.; Samdani, A.; Economides, A.; Goldman, S. A. Induction of Neostriatal Neurogenesis Slows Disease Progression in a Transgenic Murine Model of Huntington Disease. *J. Clin. Invest.* **2007**, *117*, 2889–2902.
11. Mishra, S.; Palanivelu, K. The Effect of Curcumin (Turmeric) on Alzheimer's Disease: An Overview. *Ann. Indian Acad. Neurol.* **2008**, *11*, 13–19.
12. Darvesh, A. S.; Carroll, R. T.; Bishayee, A.; Novotny, N. A.; Geldenhuys, W. J.; Van der Schyf, C. J. Curcumin and Neurodegenerative Diseases: A Perspective. *Expert Opin. Investig. Drugs* **2012**, *21*, 1123–1140.
13. Mythri, R. B.; Bharath, M. M. Curcumin: A Potential Neuroprotective Agent in Parkinson's Disease. *Curr. Pharm. Des.* **2012**, *18*, 91–99.
14. Hickey, M. A.; Zhu, C.; Medvedeva, V.; Lerner, R. P.; Patassini, S.; Franich, N. R.; Maiti, P.; Frautschy, S. A.; Zeitlin, S.; Levine, M. S.; *et al.* Improvement of Neuropathology and Transcriptional Deficits in Cag 140 Knock-in Mice Supports a Beneficial Effect of Dietary Curcumin in Huntington's Disease. *Mol. Neurodegener.* **2012**, *7*, 12.
15. Xie, L.; Li, X. K.; Takahara, S. Curcumin Has Bright Prospects for the Treatment of Multiple Sclerosis. *Int. Immunopharmacol.* **2011**, *11*, 323–330.
16. Bishnoi, M.; Chopra, K.; Kulkarni, S. K. Protective Effect of Curcumin, the Active Principle of Turmeric (Curcuma Longa)

in Haloperidol-Induced Orofacial Dyskinesia and Associated Behavioural, Biochemical and Neurochemical Changes in Rat Brain. *Pharmacol., Biochem. Behav.* **2008**, *88*, 511–522.
17. Yang, C.; Zhang, X.; Fan, H.; Liu, Y. Curcumin Upregulates Transcription Factor Nrf2, Ho-1 Expression and Protects Rat Brains against Focal Ischemia. *Brain Res.* **2009**, *1282*, 133–141.
18. Szwed, A.; Milowska, K. The Role of Proteins in Neurodegenerative Disease. *Postepy Hig. Med. Dosw.* **2012**, *66*, 187–195.
19. Ahmed, T.; Enam, S. A.; Gilani, A. H. Curcuminoids Enhance Memory in an Amyloid-Infused Rat Model of Alzheimer's Disease. *Neuroscience* **2010**, *169*, 1296–1306.
20. Liao, K. K.; Wu, M. J.; Chen, P. Y.; Huang, S. W.; Chiu, S. J.; Ho, C. T.; Yen, J. H. Curcuminoids Promote Neurite Outgrowth in Pc12 Cells through Mapk/Erk- and Pkc-Dependent Pathways. *J. Agric. Food Chem.* **2012**, *60*, 433–443.
21. Kim, S. J.; Son, T. G.; Park, H. R.; Park, M.; Kim, M. S.; Kim, H. S.; Chung, H. Y.; Mattson, M. P.; Lee, J. Curcumin Stimulates Proliferation of Embryonic Neural Progenitor Cells and Neurogenesis in the Adult Hippocampus. *J. Biol. Chem.* **2008**, *283*, 14497–14505.
22. Xu, Y.; Ku, B.; Cui, L.; Li, X.; Barish, P. A.; Foster, T. C.; Ogle, W. O. Curcumin Reverses Impaired Hippocampal Neurogenesis and Increases Serotonin Receptor 1a mRNA and Brain-Derived Neurotrophic Factor Expression in Chronically Stressed Rats. *Brain Res.* **2007**, *1162*, 9–18.
23. Dong, S.; Zeng, Q.; Mitchell, E. S.; Xiu, J.; Duan, Y.; Li, C.; Tiwari, J. K.; Hu, Y.; Cao, X.; Zhao, Z. Curcumin Enhances Neurogenesis and Cognition in Aged Rats: Implications for Transcriptional Interactions Related to Growth and Synaptic Plasticity. *PLoS One* **2012**, *7*, e31211.
24. Kang, S. K.; Cha, S. H.; Jeon, H. G. Curcumin-Induced Histone Hypoacetylation Enhances Caspase-3-Dependent Glioma Cell Death and Neurogenesis of Neural Progenitor Cells. *Stem Cells Dev.* **2006**, *15*, 165–174.
25. Tsai, Y. M.; Chien, C. F.; Lin, L. C.; Tsai, T. H. Curcumin and Its Nano-Formulation: The Kinetics of Tissue Distribution and Blood-Brain Barrier Penetration. *Int. J. Pharm.* **2011**, *416*, 331–338.
26. Vergoni, A. V.; Tosi, G.; Tacchi, R.; Vandelli, M. A.; Bertolini, A.; Costantino, L. Nanoparticles as Drug Delivery Agents Specific for CNS: *In Vivo* Biodistribution. *Nanomedicine* **2009**, *5*, 369–377.
27. Reddy, M. K.; Labhasetwar, V. Nanoparticle-Mediated Delivery of Superoxide Dismutase to the Brain: An Effective Strategy to Reduce Ischemia-Reperfusion Injury. *FASEB J.* **2009**, *23*, 1384–1395.
28. Tiwari, M. N.; Agarwal, S.; Bhatnagar, P.; Singhal, N. K.; Tiwari, S. K.; Kumar, P.; Chauhan, L. K.; Patel, D. K.; Chaturvedi, R. K.; Singh, M. P.; *et al*. Nicotine-Encapsulated Poly-(Lactic-Co-Glycolic) Acid Nanoparticles Improve Neuroprotective Efficacy against Mptp-Induced Parkinsonism. *Free Radical Biol. Med.* **2013**, *65C*, 704–718.
29. Hoppe, J. B.; Coradini, K.; Frozza, R. L.; Oliveira, C. M.; Meneghetti, A. B.; Bernardi, A.; Pires, E. S.; Beck, R. C.; Salbego, C. G. Free and Nanoencapsulated Curcumin Suppress Beta-Amyloid-Induced Cognitive Impairments in Rats: Involvement of Bdnf and Akt/Gsk-3beta Signaling Pathway. *Neurobiol. Learn. Mem.* **2013**, *106C*, 134–144.
30. Machon, O.; van den Bout, C. J.; Backman, M.; Kemler, R.; Krauss, S. Role of Beta-Catenin in the Developing Cortical and Hippocampal Neuroepithelium. *Neuroscience* **2003**, *122*, 129–143.
31. Lie, D. C.; Colamarino, S. A.; Song, H. J.; Desire, L.; Mira, H.; Consiglio, A.; Lein, E. S.; Jessberger, S.; Lansford, H.; Dearie, A. R.; *et al*. Wnt Signalling Regulates Adult Hippocampal Neurogenesis. *Nature* **2005**, *437*, 1370–1375.
32. Kuwabara, T.; Hsieh, J.; Muotri, A.; Yeo, G.; Warashina, M.; Lie, D. C.; Moore, L.; Nakashima, K.; Asashima, M.; Gage, F. H. Wnt-Mediated Activation of Neurod1 and Retro-Elements during Adult Neurogenesis. *Nat. Neurosci.* **2009**, *12*, 1097–1105.
33. Kalani, M. Y.; Cheshier, S. H.; Cord, B. J.; Bababeygy, S. R.; Vogel, H.; Weissman, I. L.; Palmer, T. D.; Nusse, R. Wnt-Mediated Self-Renewal of Neural Stem/Progenitor Cells. *Proc. Natl. Acad. Sci. U.S.A.* **2008**, *105*, 16970–16975.
34. Michaelidis, T. M.; Lie, D. C. Wnt Signaling and Neural Stem Cells: Caught in the Wnt Web. *Cell Tissue Res.* **2008**, *331*, 193–210.
35. Muroyama, Y.; Kondoh, H.; Takada, S. Wnt Proteins Promote Neuronal Differentiation in Neural Stem Cell Culture. *Biochem. Biophys. Res. Commun.* **2004**, *313*, 915–921.
36. Toledo, E. M.; Colombres, M.; Inestrosa, N. C. Wnt Signaling in Neuroprotection and Stem Cell Differentiation. *Prog. Neurobiol.* **2008**, *86*, 281–296.
37. Inestrosa, N. C.; Arenas, E. Emerging Roles of Wnts in the Adult Nervous System. *Nat. Rev. Neurosci.* **2010**, *11*, 77–86.
38. Yun, X.; Maximov, V. D.; Yu, J.; Zhu, H.; Vertegel, A. A.; Kindy, M. S. Nanoparticles for Targeted Delivery of Antioxidant Enzymes to the Brain after Cerebral Ischemia and Reperfusion Injury. *J. Cereb. Blood Flow. Metab.* **2013**, *33*, 583–592.
39. Maia, J.; Santos, T.; Aday, S.; Agasse, F.; Cortes, L.; Malva, J. O.; Bernardino, L.; Ferreira, L. Controlling the Neuronal Differentiation of Stem Cells by the Intracellular Delivery of Retinoic Acid-Loaded Nanoparticles. *ACS Nano* **2011**, *5*, 97–106.
40. Santos, T.; Ferreira, R.; Maia, J.; Agasse, F.; Xapelli, S.; Cortes, L.; Braganca, J.; Malva, J. O.; Ferreira, L.; Bernardino, L. Polymeric Nanoparticles to Control the Differentiation of Neural Stem Cells in the Subventricular Zone of the Brain. *ACS Nano* **2012**, *6*, 10463–10474.
41. Lemkine, G. F.; Mantero, S.; Migne, C.; Raji, A.; Goula, D.; Normandie, P.; Levi, G.; Demeneix, B. A. Preferential Transfection of Adult Mouse Neural Stem Cells and Their Immediate Progeny *in Vivo* with Polyethylenimine. *Mol. Cell. Neurosci.* **2002**, *19*, 165–174.
42. Doggui, S.; Sahni, J. K.; Arseneault, M.; Dao, L.; Ramassamy, C. Neuronal Uptake and Neuroprotective Effect of Curcumin-Loaded Plga Nanoparticles on the Human Sk-N-Sh Cell Line. *J. Alzheimers Dis.* **2012**, *30*, 377–392.
43. Sahay, G.; Alakhova, D. Y.; Kabanov, A. V. Endocytosis of Nanomedicines. *J. Controlled Release* **2010**, *145*, 182–195.
44. Sawicka, A.; Seiser, C. Histone H3 Phosphorylation - a Versatile Chromatin Modification for Different Occasions. *Biochimie* **2012**, *94*, 2193–2201.
45. Massalini, S.; Pellegatta, S.; Pisati, F.; Finocchiaro, G.; Farace, M. G.; Ciafre, S. A. Reelin Affects Chain-Migration and Differentiation of Neural Precursor Cells. *Mol. Cell. Neurosci.* **2009**, *42*, 341–349.
46. Knuesel, I. Reelin-Mediated Signaling in Neuropsychiatric and Neurodegenerative Diseases. *Prog. Neurobiol.* **2010**, *91*, 257–274.
47. Park, D.; Xiang, A. P.; Mao, F. F.; Zhang, L.; Di, C. G.; Liu, X. M.; Shao, Y.; Ma, B. F.; Lee, J. H.; Ha, K. S.; *et al*. Nestin Is Required for the Proper Self-Renewal of Neural Stem Cells. *Stem Cells* **2010**, *28*, 2162–2171.
48. Zhang, X.; Huang, C. T.; Chen, J.; Pankratz, M. T.; Xi, J.; Li, J.; Yang, Y.; Lavaute, T. M.; Li, X. J.; Ayala, M.; *et al*. Pax6 Is a Human Neuroectoderm Cell Fate Determinant. *Cell Stem Cell* **2010**, *7*, 90–100.
49. Kallur, T.; Gisler, R.; Lindvall, O.; Kokaia, Z. Pax6 Promotes Neurogenesis in Human Neural Stem Cells. *Mol. Cell. Neurosci.* **2008**, *38*, 616–628.
50. Maekawa, M.; Takashima, N.; Arai, Y.; Nomura, T.; Inokuchi, K.; Yuasa, S.; Osumi, N. Pax6 Is Required for Production and Maintenance of Progenitor Cells in Postnatal Hippocampal Neurogenesis. *Genes Cells* **2005**, *10*, 1001–1014.
51. Nacher, J.; Varea, E.; Blasco-Ibanez, J. M.; Castillo-Gomez, E.; Crespo, C.; Martinez-Guijarro, F. J.; McEwen, B. S. Expression of the Transcription Factor Pax 6 in the Adult Rat Dentate Gyrus. *J. Neurosci. Res.* **2005**, *81*, 753–761.
52. Sun, Y.; Nadal-Vicens, M.; Misono, S.; Lin, M. Z.; Zubiaga, A.; Hua, X.; Fan, G.; Greenberg, M. E. Neurogenin Promotes Neurogenesis and Inhibits Glial Differentiation by Independent Mechanisms. *Cell* **2001**, *104*, 365–376.
53. Roybon, L.; Hjalt, T.; Stott, S.; Guillemot, F.; Li, J. Y.; Brundin, P. Neurogenin2 Directs Granule Neuroblast Production and Amplification While Neurod1 Specifies Neuronal Fate

during Hippocampal Neurogenesis. *PLoS One* **2009**, *4*, e4779.
54. Gu, F.; Hata, R.; Ma, Y. J.; Tanaka, J.; Mitsuda, N.; Kumon, Y.; Hanakawa, Y.; Hashimoto, K.; Nakajima, K.; Sakanaka, M. Suppression of Stat3 Promotes Neurogenesis in Cultured Neural Stem Cells. *J. Neurosci. Res.* **2005**, *81*, 163–171.
55. Cao, F.; Hata, R.; Zhu, P.; Nakashiro, K.; Sakanaka, M. Conditional Deletion of Stat3 Promotes Neurogenesis and Inhibits Astrogliogenesis in Neural Stem Cells. *Biochem. Biophys. Res. Commun.* **2010**, *394*, 843–847.
56. Seib, D. R.; Corsini, N. S.; Ellwanger, K.; Plaas, C.; Mateos, A.; Pitzer, C.; Niehrs, C.; Celikel, T.; Martin-Villalba, A. Loss of Dickkopf-1 Restores Neurogenesis in Old Age and Counteracts Cognitive Decline. *Cell Stem Cell* **2013**, *12*, 204–214.
57. Yoshinaga, Y.; Kagawa, T.; Shimizu, T.; Inoue, T.; Takada, S.; Kuratsu, J.; Taga, T. Wnt3a Promotes Hippocampal Neurogenesis by Shortening Cell Cycle Duration of Neural Progenitor Cells. *Cell. Mol. Neurobiol.* **2010**, *30*, 1049–1058.
58. Zhang, L.; Yang, X.; Yang, S.; Zhang, J. The Wnt /Beta-Catenin Signaling Pathway in the Adult Neurogenesis. *Eur. J. Neurosci.* **2011**, *33*, 1–8.
59. Castelo-Branco, G.; Wagner, J.; Rodriguez, F. J.; Kele, J.; Sousa, K.; Rawal, N.; Pasolli, H. A.; Fuchs, E.; Kitajewski, J.; Arenas, E. Differential Regulation of Midbrain Dopaminergic Neuron Development by Wnt-1, Wnt-3a, and Wnt-5a. *Proc. Natl. Acad. Sci. U.S.A.* **2003**, *100*, 12747–12752.
60. Castelo-Branco, G.; Sousa, K. M.; Bryja, V.; Pinto, L.; Wagner, J.; Arenas, E. Ventral Midbrain Glia Express Region-Specific Transcription Factors and Regulate Dopaminergic Neurogenesis through Wnt-5a Secretion. *Mol. Cell. Neurosci.* **2006**, *31*, 251–262.
61. Paina, S.; Garzotto, D.; DeMarchis, S.; Marino, M.; Moiana, A.; Conti, L.; Cattaneo, E.; Perera, M.; Corte, G.; Calautti, E.; *et al*. Wnt5a Is a Transcriptional Target of Dlx Homeogenes and Promotes Differentiation of Interneuron Progenitors *in Vitro* and *in Vivo*. *J. Neurosci.* **2011**, *31*, 2675–2687.
62. Andersson, E. R.; Salto, C.; Villaescusa, J. C.; Cajanek, L.; Yang, S.; Bryjova, L.; Nagy, I. I.; Vainio, S. J.; Ramirez, C.; Bryja, V.; *et al*. Wnt5a Cooperates with Canonical Wnts to Generate Midbrain Dopaminergic Neurons *in Vivo* and in Stem Cells. *Proc. Natl. Acad. Sci. U.S.A.* **2013**, *110*, E602–610.
63. Okamoto, M.; Inoue, K.; Iwamura, H.; Terashima, K.; Soya, H.; Asashima, M.; Kuwabara, T. Reduction in Paracrine Wnt3 Factors during Aging Causes Impaired Adult Neurogenesis. *FASEB J.* **2011**, *25*, 3570–3582.
64. Favaro, R.; Valotta, M.; Ferri, A. L.; Latorre, E.; Mariani, J.; Giachino, C.; Lancini, C.; Tosetti, V.; Ottolenghi, S.; Taylor, V.; *et al*. Hippocampal Development and Neural Stem Cell Maintenance Require Sox2-Dependent Regulation of Shh. *Nat. Neurosci.* **2009**, *12*, 1248–1256.
65. Lee, S. M.; Tole, S.; Grove, E.; McMahon, A. P. A Local Wnt-3a Signal Is Required for Development of the Mammalian Hippocampus. *Development* **2000**, *127*, 457–467.
66. Spaccapelo, L.; Galantucci, M.; Neri, L.; Contri, M.; Pizzala, R.; D'Amico, R.; Ottani, A.; Sandrini, M.; Zaffe, D.; Giuliani, D.; *et al*. Up-Regulation of the Canonical Wnt-3a and Sonic Hedgehog Signaling Underlies Melanocortin-Induced Neurogenesis after Cerebral Ischemia. *Eur. J. Pharmacol.* **2013**, *707*, 78–86.
67. Pinnock, S. B.; Blake, A. M.; Platt, N. J.; Herbert, J. The Roles of Bdnf, Pcreb and Wnt3a in the Latent Period Preceding Activation of Progenitor Cell Mitosis in the Adult Dentate Gyrus by Fluoxetine. *PLoS One* **2010**, *5*, e13652.
68. Ahn, J.; Lee, H.; Kim, S.; Ha, T. Curcumin-Induced Suppression of Adipogenic Differentiation Is Accompanied by Activation of Wnt/Beta-Catenin Signaling. *Am. J. Physiol.* **2010**, *298*, C1510–1516.
69. Ding, S.; Wu, T. Y.; Brinker, A.; Peters, E. C.; Hur, W.; Gray, N. S.; Schultz, P. G. Synthetic Small Molecules That Control Stem Cell Fate. *Proc. Natl. Acad. Sci. U.S.A.* **2003**, *100*, 7632–7637.
70. Geng, X.; Xiao, L.; Lin, G. F.; Hu, R.; Wang, J. H.; Rupp, R. A.; Ding, X. Lef/Tcf-Dependent Wnt/Beta-Catenin Signaling during Xenopus Axis Specification. *FEBS Lett.* **2003**, *547*, 1–6.
71. Zhang, X.; Yin, W. K.; Shi, X. D.; Li, Y. Curcumin Activates Wnt/Beta-Catenin Signaling Pathway through Inhibiting the Activity of Gsk-3beta in Appswe Transfected Sy5y Cells. *Eur. J. Pharm. Sci.* **2011**, *42*, 540–546.
72. Piao, S.; Lee, S. H.; Kim, H.; Yum, S.; Stamos, J. L.; Xu, Y.; Lee, S. J.; Lee, J.; Oh, S.; Han, J. K.; *et al*. Direct Inhibition of Gsk3beta by the Phosphorylated Cytoplasmic Domain of Lrp6 in Wnt/Beta-Catenin Signaling. *PLoS One* **2008**, *3*, e4046.
73. Grumolato, L.; Liu, G.; Mong, P.; Mudbhary, R.; Biswas, R.; Arroyave, R.; Vijayakumar, S.; Economides, A. N.; Aaronson, S. A. Canonical and Noncanonical Wnts Use a Common Mechanism to Activate Completely Unrelated Coreceptors. *Genes Dev.* **2010**, *24*, 2517–2530.
74. MacDonald, B. T.; Tamai, K.; He, X. Wnt/Beta-Catenin Signaling: Components, Mechanisms, and Diseases. *Dev. Cell* **2009**, *17*, 9–26.
75. Cselenyi, C. S.; Jernigan, K. K.; Tahinci, E.; Thorne, C. A.; Lee, L. A.; Lee, E. Lrp6 Transduces a Canonical Wnt Signal Independently of Axin Degradation by Inhibiting Gsk3's Phosphorylation of Beta-Catenin. *Proc. Natl. Acad. Sci. U.S.A.* **2008**, *105*, 8032–8037.
76. McManus, E. J.; Sakamoto, K.; Armit, L. J.; Ronaldson, L.; Shpiro, N.; Marquez, R.; Alessi, D. R. Role That Phosphorylation of Gsk3 Plays in Insulin and Wnt Signalling Defined by Knockin Analysis. *EMBO J.* **2005**, *24*, 1571–1583.
77. Wisniewska, M. B. Physiological Role of Beta-Catenin/Tcf Signaling in Neurons of the Adult Brain. *Neurochem. Res.* **2013**, *38*, 1144–1155.
78. Hoppe, J. B.; Frozza, R. L.; Pires, E. N.; Meneghetti, A. B.; Salbego, C. The Curry Spice Curcumin Attenuates Beta-Amyloid-Induced Toxicity through Beta-Catenin and Pi3k Signaling in Rat Organotypic Hippocampal Slice Culture. *Neurol. Res.* **2013**, *35*, 857–866.
79. Zheng, M.; Liu, J.; Ruan, Z.; Tian, S.; Ma, Y.; Zhu, J.; Li, G. Intrahippocampal Injection of Abeta1−42 Inhibits Neurogenesis and Down-Regulates Ifn-Gamma and Nf-Kappab Expression in Hippocampus of Adult Mouse Brain. *Amyloid* **2013**, *20*, 13–20.
80. He, P.; Shen, Y. Interruption of Beta-Catenin Signaling Reduces Neurogenesis in Alzheimer's Disease. *J. Neurosci.* **2009**, *29*, 6545–6557.
81. Fiorentini, A.; Rosi, M. C.; Grossi, C.; Luccarini, I.; Casamenti, F. Lithium Improves Hippocampal Neurogenesis, Neuropathology and Cognitive Functions in App Mutant Mice. *PLoS One* **2010**, *5*, e14382.
82. Toledo, E. M.; Inestrosa, N. C. Activation of Wnt Signaling by Lithium and Rosiglitazone Reduced Spatial Memory Impairment and Neurodegeneration in Brains of an Appswe/Psen1deltae9Mouse Model of Alzheimer's Disease. *Mol. Psychiatry* **2010**, *15* (272−285), 228.
83. Mathew, A.; Fukuda, T.; Nagaoka, Y.; Hasumura, T.; Morimoto, H.; Yoshida, Y.; Maekawa, T.; Venugopal, K.; Kumar, D. S. Curcumin Loaded-Plga Nanoparticles Conjugated with Tet-1 Peptide for Potential Use in Alzheimer's Disease. *PLoS One* **2010**, *7*, e32616.
84. Malinauskas, T.; Aricescu, A. R.; Lu, W.; Siebold, C.; Jones, E. Y. Modular Mechanism of Wnt Signaling Inhibition by Wnt Inhibitory Factor 1. *Nat. Struct. Mol. Biol.* **2011**, *18*, 886–893.
85. Kawano, Y.; Kypta, R. Secreted Antagonists of the Wnt Signalling Pathway. *J. Cell Sci.* **2003**, *116*, 2627–2634.
86. Cohen, P.; Goedert, M. Gsk3 Inhibitors: Development and Therapeutic Potential. *Nat. Rev. Drug Discovery* **2004**, *3*, 479–487.
87. Swami, A.; Aggarwal, A.; Pathak, A.; Patnaik, S.; Kumar, P.; Singh, Y.; Gupta, K. C. Imidazolyl-Pei Modified Nanoparticles for Enhanced Gene Delivery. *Int. J. Pharm.* **2007**, *335*, 180–192.
88. Asadishad, B.; Vossoughi, M.; Alamzadeh, I. *In Vitro* Release Behavior and Cytotoxicity of Doxorubicin-Loaded Gold Nanoparticles in Cancerous Cells. *Biotechnol. Lett.* **2010**, *32*, 649–654.
89. Agrawal, A. K.; Chaturvedi, R. K.; Shukla, S.; Seth, K.; Chauhan, S.; Ahmad, A.; Seth, P. K. Restorative Potential

of Dopaminergic Grafts in Presence of Antioxidants in Rat Model of Parkinson's Disease. *J. Chem. Neuroanat.* **2004**, *28*, 253–264.
90. Mishra, D.; Tiwari, S. K.; Agarwal, S.; Sharma, V. P.; Chaturvedi, R. K. Prenatal Carbofuran Exposure Inhibits Hippocampal Neurogenesis and Causes Learning and Memory Deficits in Offspring. *Toxicol. Sci.* **2012**, *127*, 84–100.
91. Chiu, S. S.; Lui, E.; Majeed, M.; Vishwanatha, J. K.; Ranjan, A. P.; Maitra, A.; Pramanik, D.; Smith, J. A.; Helson, L. Differential Distribution of Intravenous Curcumin Formulations in the Rat Brain. *Anticancer Res.* **2011**, *31*, 907–911.
92. Wennstrom, M.; Hellsten, J.; Ekstrand, J.; Lindgren, H.; Tingstrom, A. Corticosterone-Induced Inhibition of Gliogenesis in Rat Hippocampus Is Counteracted by Electroconvulsive Seizures. *Biol. Psychiatry* **2006**, *59*, 178–186.
93. Martinez-Canabal, A.; Akers, K. G.; Josselyn, S. A.; Frankland, P. W. Age-Dependent Effects of Hippocampal Neurogenesis Suppression on Spatial Learning. *Hippocampus* **2013**, *23*, 66–74.
94. Schmued, L. C.; Hopkins, K. J.; Fluoro-Jade, B.; High, A. Affinity Fluorescent Marker for the Localization of Neuronal Degeneration. *Brain Res.* **2000**, *874*, 123–130.